Fisheries New Zealand

Tini a Tangaroa

Abundance and Distribution of Hector's dolphin on South Coast South Island

New Zealand Government

Requests for further copies should be directed to:

Publications Logistics Officer
Ministry for Primary Industries
PO Box 2526
WELLINGTON 6140

Email: brand@mpi.govt.nz
Telephone: 0800 00 83 33
Facsimile: 04-894 0300

This publication is also available on the Ministry for Primary Industries websites at:
http://www.mpi.govt.nz/news-and-resources/publications
http://fs.fish.govt.nz go to Document library/Research reports

TABLE OF CONTENTS

EXECUTIVE SUMMARY

MacKenzie, D.I.; Clement, D.M. (2019). Abundance and distribution of Hector's dolphin on South Coast South Island.
New Zealand Aquatic Environment and Biodiversity Report No. 236. **44 p.**

Fisheries New Zealand and the Department of Conservation are currently reviewing the Hector's dolphin Threat Management Plan. As the previous south coast of the South Island (SCSI) abundance estimate is now eight years old, an updated abundance and distribution estimate is necessary for this review. This study constitutes the final abundance estimate of the three regional Hector's dolphin sub-populations; ECSI aerial surveys in 2013 and WCSI aerial surveys in 2015.

A summer survey programme was specifically designed for sampling the expected low SCSI population size using a simulation study based on the previous 2010 SCSI aerial survey results. This design recommended five replicate surveys be undertaken in the higher-density area of Te Waewae Bay. The SCSI survey area (6139 km^2) between Long Point, Fiordland and Nugget Point, Otago was stratified into five coastal sections for line orientation and into two offshore substrata to encompass the dolphins' offshore distribution. Double observer, line-transect methodology was used with transect lines orientated in the offshore direction and spaced parallel at equal intervals using systematic-random line placement.

Hector's dolphin abundance was estimated using mark-recapture distance sampling (MRDS) techniques that allow for a lack of independence between the observer detections. Availability bias is a fundamentally important component for obtaining a reliable estimate of total abundance. While two different methods were used to assess Hector's dolphin surface availability along the ECSI and WSCI surveys, only helicopter methods were undertaken in SCSI due to low population abundance and therefore, an expected lack of opportunity to undertake a sufficient number of circle-backs.

Summer surveys resulted in 75 dolphin groups (28 of which were seen by two observers) sighted between 0.04 km and 0.3 km either side of the plane, along 2574 km of transect lines. All 75 sightings used in the analysis were observed in Te Waewae Bay, fairly close to shore and within relatively shallow depths (less than 30 m). There was only one sighting outside of Te Waewae Bay, off Toetoes Bay, but it was beyond 0.3 km from the plane, so was excluded from the analysis.

The availability estimate (length of time a dolphin group would be in an observer's field of view, *t*=6 seconds), was 0.61. This estimate is similar to the reanalysed estimates of 0.57 for March and 0.67 for August from the 2010 survey.

The SCSI Hector's dolphin summer abundance was estimated to be 332 animals (CV: 22%; 95% CI 217–508). These estimates are in good agreement with the previous 2010 SCSI reanalysed estimate of 238 (CV: 40%; 95% CI: 113–503). The improvement in the precision of the current estimate is likely to be due to a greater number of on-effort group sightings during the survey and close to that expected from pre-survey simulations using the proposed design.

Abundance estimates have not been given for the areas other than Te Waewae Bay due to there being no qualifying sightings. However, we stress that the lack of an estimate should not be interpreted as indicating that Hector's dolphin are entirely absent from these strata. We strongly suspect that there are Hector's dolphin in those strata, but at such low density that our survey effort was insufficient to detect them.

1. INTRODUCTION

Hector's dolphin, *Cephalorhynchus hectori hectori*, is only found within New Zealand waters and is currently listed as *Nationally Endangered* by the NZ threat classification scheme (Baker et al. 2010) and considered *Endangered* by the IUCN since 2000 (Reeves et al. 2008). From a series of aerial surveys conducted from 2013–2015, the population of this species around the South Island has been estimated at approximately 14 849 animals (CV: 11%, 95% CI: 11 923–18 492; MacKenzie & Clement 2016b).

MPI and DOC have agreed to undertake a review of the Hector's Dolphin Threat Management Plan in 2018 as this species' coastal distribution significantly overlaps with inshore setnet and trawl fisheries (DOC & MFish 2007). As part of this process, decision-makers must take into account sections 8, 9, and 15 of the Fisheries Act 1996, which include guidance to avoid, remedy or mitigate any adverse effects of fishing on the aquatic environment, including the effects of fishing related mortality on protected species. For this review, an up-to-date abundance estimate of Hector's dolphin is required as the previous 1997–2001 estimate was too old for management purposes and more recent research demonstrates that this species ranges further offshore than previous abundance surveys have sampled (e.g. DuFresne & Mattlin 2009, Rayment et al. 2010a).

1.1 Background

The South Island population of Hector's dolphin is clumped, geographically and genetically, into three fairly distinct sub-populations (Dawson & Slooten 1988, Pichler et al. 1998, Hamner et al. 2012). Based on previous estimates (Slooten et al. 2004), the majority of dolphins (about 3600 to 8000) were thought to occur along the West Coast (WCSI; between Farewell Spit and Milford Sound) with the remainder found along the East Coast (ESCI; from Farewell Spit to Nugget Point) and South Coast (SCSI; from Nugget Point to Long Point).

This abundance estimate is based on a series of four surveys, three undertaken by boat and one by airplane, over four consecutive summer seasons between 1997/1998 and 2000/2001. All four surveys were based on line-transect sampling methods and targeted the inshore waters between the coastline and four nautical miles (nmi) offshore. Sparse sampling effort was allocated to more offshore regions as previous research (Dawson & Slooten 1988) suggested that few dolphins occurred beyond four nmi offshore. As a result, abundance was not estimated for more offshore waters (Dawson et al. 2004, Slooten et al. 2004).

In 2008, the Ministry of Fisheries and Department of Conservation (DOC) released a draft Hector's and Maui's Dolphin Threat Management Plan (TMP). This management document highlighted fishing-related mortalities as one of the main human-induced, yet highly uncertain, threats to this species. To mitigate such effects, the TMP established a range of fisheries prohibited zones and several non-fisheries protective measures throughout the three sub-populations based on the above abundance estimates and all available data (DOC & MFish 2007). These measures focused on the waters out to four nmi where the majority of dolphins occur and overlap with both commercial and recreational setnet fisheries and inshore trawl fisheries.

Since the abundance surveys were completed and the TMP measures implemented, additional aerial-based studies have been undertaken within several localised regions around the South Island (i.e. DuFresne & Mattlin 2009, DuFresne et al. 2010, Rayment et al. 2010a, 2010b, Clement et al. 2011). There are several advantages to using aerial platforms for research on Hector's dolphins. The biggest advantages include being able to synoptically sample a large

study area in much shorter time periods than boat platforms, which minimises the effect of any directional or seasonal movement while also eliciting little to no responsive behaviours from the dolphins (Slooten et al. 2004).

All of these studies found Hector's dolphin regularly occurring past four nmi and some much further offshore than it was previously thought that this species might normally occur (e.g. 16 nmi DuFresne & Mattlin 2009; 18 nmi Rayment et al. 2010a). In addition, recent abundance surveys along the east and north coasts (MacKenzie & Clement 2014) indicated much larger regional populations of Hector's dolphins present over summer than the previous abundance survey estimated (Slooten et al. 2004). These findings suggest that the 1997–2001 abundance survey may have missed a proportion of dolphins from these offshore regions and that the overall population of Hector's dolphin is likely to be larger than previously estimated.

1.2   Scope

The Cawthron Institute (Cawthron), in conjunction with Proteus Wildlife Research Consultants (Proteus), were contracted by MPI to conduct an aerial survey along the SCSI during the summer months of 2018. The resulting survey programme was designed specifically for the SCSI population and based on previous aerial methods for this species (MacKenzie & Clement 2014, 2016). The previous design work for the ECSI survey (under contract PRO2009/01B) identified inconsistencies in how sightings of dolphin groups within the observer overlap zone have been incorporated in the detection function analysis when estimating Hector's dolphin abundance by different researchers. As a result, the earlier SCSI aerial surveys (Clement et al. 2011) were reanalysed using the same general approach to the detection function modelling as that used for the ECSI and WCSI analyses in order to calculate a combined South Island population estimate for Hector's dolphins. This reanalysis indicated that the population may be smaller than previously thought (238 individuals; CV: 40%; 95% CI: 113–503).

Given that abundance estimate is now eight years old, an updated abundance and distribution estimate is necessary ahead of the 2018 review of the TMP. This study constitutes the last abundance estimate of the three regional Hector's dolphin sub-populations; following on from the ECSI aerial surveys in 2013 (MacKenzie & Clement 2014) and WCSI aerial surveys in 2015 (MacKenzie & Clement 2016 b,c). The specific scope of this programme is outlined as follows.

Overall Objective:

To estimate the abundance and distribution of the South Coast South Island population of Hector's dolphins to enable assessments of population status, trends and the effects of fishing-related mortality on this population.

Specific Objectives:

1. To develop and refine design and methods for summer surveys for Hector's dolphins along the SCSI.
2. To estimate the abundance of Hector's dolphins along the SCSI applying an agreed survey and analysis methodology.
3. To estimate the distribution of Hector's dolphins along the SCSI applying an agreed survey and analysis methodology.

2. METHODS

For Objectives 1–3, the survey programme was based on the general aerial survey design outlined in MacKenzie et al. (2012) as they have been previous applied and refined on the ECSI and WCSI surveys (MacKenzie & Clement 2016a). Detailed discussions of the survey protocols and methods are provided in MacKenzie & Clement (2016b) and a summary as they have been applied to the SCSI survey is given below.

2.1 SCSI survey design and effort

The 6139 km^2 of the SCSI survey area was stratified into five coastal sections for line orientation (only three of which were used in abundance estimation) and each divided into one to two offshore substrata of 0–4 nmi (inner) and 4–20 nmi (outer – see Table 1), as agreed at the November 2017 AEWG meeting. The proposed design was evaluated using a simulation study with input parameters based on the 2010 aerial survey results (MacKenzie & Clement 2017; see Appendix 1). This design was expected to encompass the distributional limits of Hector's dolphin along the south coast as estimated by Clement et al. (2011) and aimed at achieving an abundance estimate with a CV lower than 30–40%; by allocating sampling effort to areas with a higher expected density.

A summer survey of all continuous transect lines (113 lines) was carried out between 14 February and 5 March 2018. Note that the offshore stratification subdivides many of the continuous transects, hence there was a total of 158 transect lines for the purpose of the analysis (Figure 1; i.e. one continuous transect line may be considered as two lines for analysis purposes if it spans across all of the offshore substrata). More intensive sampling was allocated within the known high-density region of Te Waewae Bay (Table 1). Less intensive sampling was carried out in suspected low-density strata, although effort was still greater than what would have been considered optimal for estimating abundance (MacKenzie et al. 2012) in recognition that little survey work has been conducted in those areas and for the dual survey objectives of estimating abundance and distribution. When appropriately designed, repeated 'on-effort' surveys that contribute to the final abundance estimate (while accounting for the increased effort in that region) is a more efficient use of resources than auxiliary 'off-effort' surveys that would only be used to estimate the shape of the detection function. Hence, the final design included approximately five replicate surveys of the Te Waewae Bay area (i.e. re-survey each line 5 times; Table 1).

Table 1:   **Summer survey line spacing with estimated and achieved levels of effort in each stratum.**

| Alongshore Stratum	Offshore Stratum	Survey Area (km²)	Line Spacing (km)	Estimated Length of Transects (per replicate km)	Proposed Replicates	Achieved Length of Transects (km)
Te Waewae Bay	Inner (0–4 nmi)	379	1.85	1 105 (221)	5	1 045
(east and west)	Middle (4–12 nmi)	151	1.85	360 (72)	5	341
Toetoes Bay	Inner (0–4 nmi)	592	1.85	307	1	309
Elsewhere	Inner (0–4 nmi)	1 558	3.70	420	1	419
	Outer (>4 nmi)	3 458	7.40	458	1	460
Total		**6 139**		**2 650 (1 478)**		**2 574**
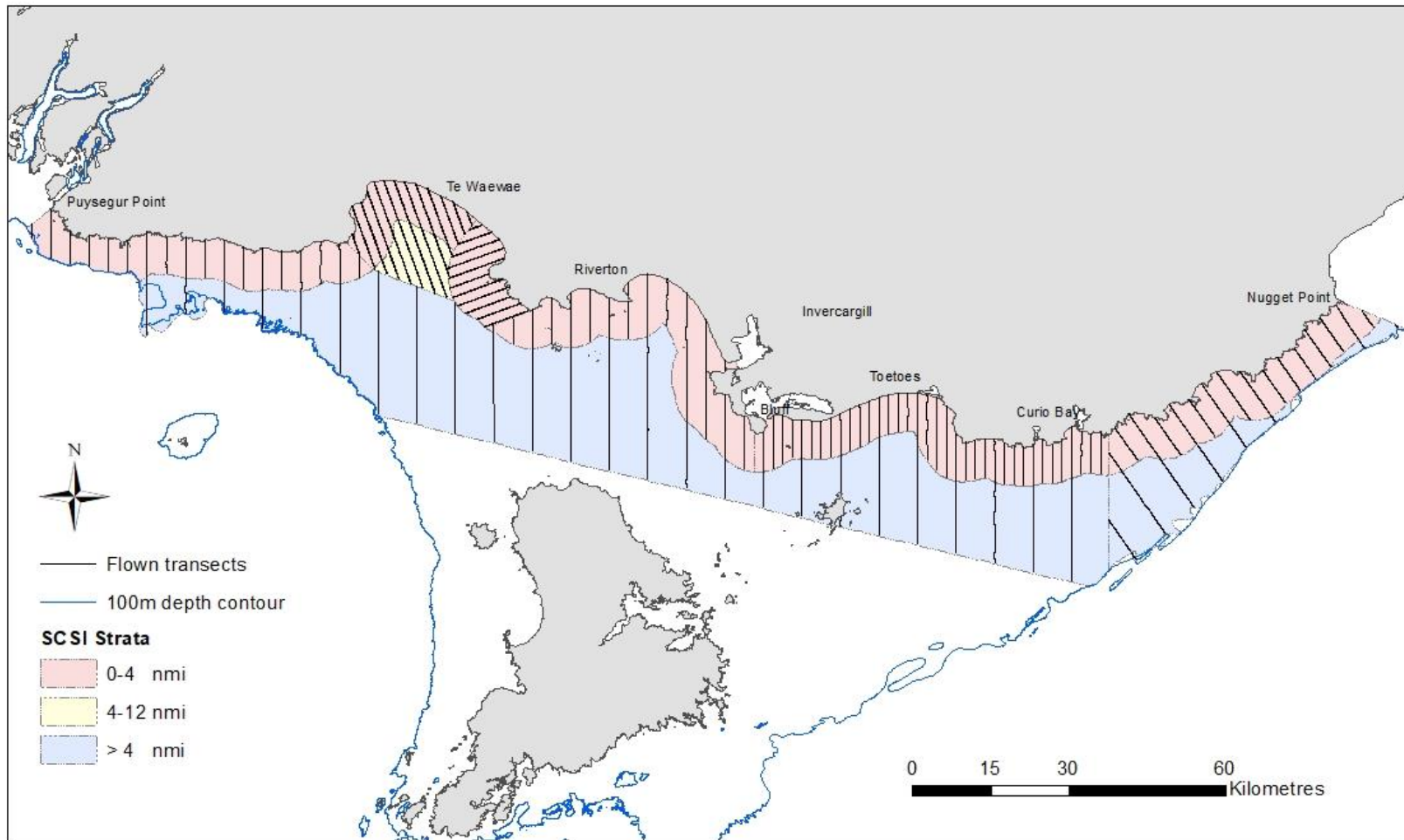
Figure 1: SCSI summer survey transects flown between 14 February and 5 March 2018.

2.2   SCSI survey platform and protocol

We used the same high-wing, Gippsland Airvan (LOR) as flown in the SCSI 2010 surveys, instead of the Cessna 207 aircraft from the ECSI 2013 and WCSI 2015 surveys as it is no longer available for survey work. While this plane still allowed for two sets of observers to independently search for Hector's dolphins, two on each side of the aircraft, it did not offer full bubble windows in which to see directly underneath the plane while surveying. Instead, three of the four observer windows had a partial bubble window configuration that was deeper than the front windows of the Cessna 207, but did not extend to 90°. The front observer window on the left side of the plane differed as it was flatter to allow for the rear door to slide open and shut. As a result, observers in the partial bubble windows (both rear and front right windows) had a search zone between the downward angles of 20°–80°, while the front left observer using the flat window had a search zone of 20°–75°.

Each observer recorded downward angle and time (to the second) of each observation into individual dictaphones, as well as other relevant sighting information (e.g. group size, presence of calves, sighting conditions). To minimise the chance of one observer visually cueing off the other, black sheets of fabric were hung between the two seats on each side of the plane. Observers were rotated amongst all positions in the aircraft such that each person spent approximately the same amount of time in each position.

Transects were surveyed at an altitude of 152.4 metres (500 feet) at a speed of approximately 100 knots (185.2 km/h). Surveys were only undertaken in suitable conditions; Beaufort sea state (Beaufort 3 or less), glare intensity (1 to 3 with no fog or obstructive clouds), and good light conditions (one hour after sunrise and before sunset). Additional sighting condition information collected included; percent glare (recorded as the proportion of the field of view obscured), glare direction, water colour (categorised as blue, blue-green, green or brown), and swell height if present.

A team of four observers was used, one of whom had participated in both the ECSI and WCSI Hector's dolphin surveys. As observers had various levels of marine mammal observing and aerial survey experience, extensive pre-survey training was conducted between 5 and 10 February 2018 off Rangiora, a high-density region for Hector's dolphins just north of Banks Peninsula. A final training day was undertaken in Te Waewae Bay on the 13 February 2018 for observers to adjust to local SCSI conditions and trial transect spacings. Training flights helped confirm the size of the fields of view for observers, ensured that observers were skilled in the field protocols and recording requirements, and helped to familiarise the pilot with the survey design, protocols and communication with observers.

Approximately 19 hours of training flights were completed, with individual observer training hours varying between 16.4 and 19.1 hrs (Table 2). Observers flew 83 transects and made 367 training sightings (Figure 2). All newly trained observers recorded at least 36 duplicate sightings with more experienced observers before surveying commenced, well over the recommended 20 sightings minimum (Dawson et al. 2008). To gauge observer performance, each observer's training sightings were compared against more experienced observers when on the same side of the plane (i.e. number of duplicate sightings versus number of experienced observer sightings within shared viewing zone only). By the end of both training periods, the detection rates of observers ranged between 70 and 75% (Table 2) of that of the more experienced observers. Training data were used for training purposes only and not included in any further analyses.

Table 2: Observer statistics from training flights off Rangiora (north of Banks Peninsula) and Te Waewae Bay (SCSI). Note – the numbering of observers is continued from the ECSI surveys (MacKenzie & Clement 2014).

|	Ob2	Ob12	Ob13	Ob14
Flying Hours	19.10	19.10	16.43	17.63
On-effort Sightings	99	91	91	65
Training Detection Rate	75%	74%	71%	76%
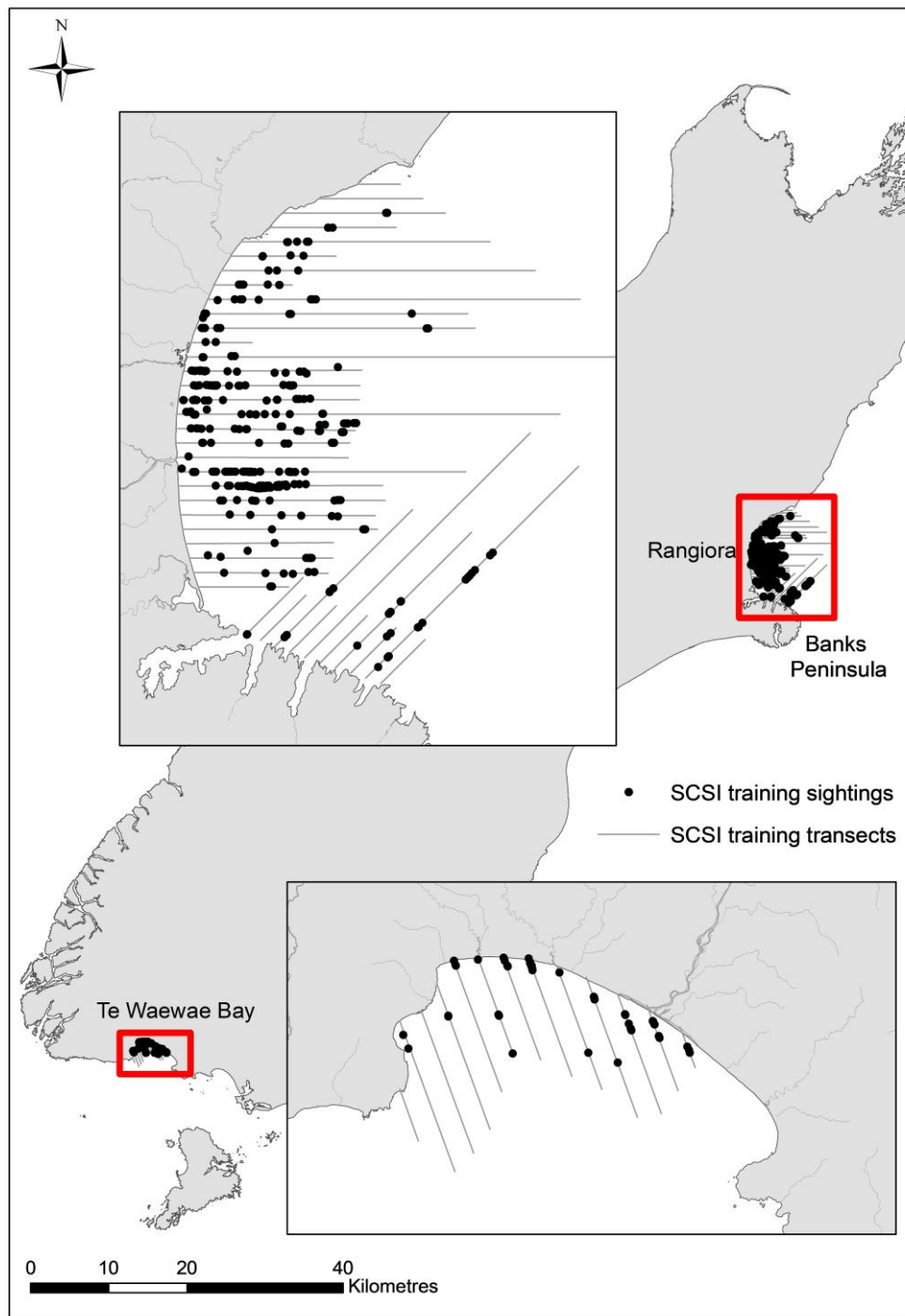
Figure 2: The locations of Hector's dolphin sightings and transects flown during observer training off Rangiora (top insert) and Te Waewae Bay (bottom inset) during 7–13 February 2018.

2.3 Abundance Analyses

Data Selection

Any sightings that were data deficient (e.g. angle not measured, seconds not heard, uncertain about species' identification) were removed prior to analysis (Table 3). A right-truncation distance of 0.3 km (27 degrees) was used for both front and rear observer positions, consistent with the truncation distance used on ECSI and WCSI (MacKenzie & Clement 2014, 2016b). A left-truncation distance of 0.04 km (75 degrees) was used for all observer positions.

Table 3: The numbers of sightings removed through data verification prior to inclusion in abundance or distribution analyses. Sightings were initially removed due to either uncertainty around species identification or missed information about the exact time or angle of the sighting. Unique sightings is the number of unique dolphin groups after matching of duplicate sightings. Additional sightings were removed as part of the left and right truncation process. Final sightings numbers represent those sightings used in the final full analyses.

	Raw sighting #	Uncertain about identification	Missed angle/time	Unique Sightings	Truncated ^	Final Sighting #
SCSI	109	6	0	80	5	**75**

^ Sightings were left truncated at 0.040 km and right truncated at 0.300 km for both observer positions.

Duplicate sightings were those in which the same group of animals was recorded by both the front and rear observer (on the same side of the plane). Duplicates were manually identified by comparing three different sighting variables; sighting time (within ± 5 seconds), sighting angle (within ± 5 degrees) and group size (± 1 individual), in line with criteria from the previous WCSI, ECSI and other Hector's dolphin aerial surveys (e.g. DuFresne & Mattlin 2009, Clement et al. 2011), as well as any distinguishing comments recorded by observers (e.g. mother/calf pair, birds nearby).

Duplicate sightings were retained in the final database as a single sighting of a group in which the average angle was used to calculate distance from the trackline, and where the recorded groups sizes differed, the larger value was retained. There were only two sightings in which group size differed by two individuals (i.e. 7% of duplicates), the rest differed by one individual (i.e. 20% of duplicates). As observers were instructed to record the minimum group size they were certain of rather than approximating group size, the larger value was used as it was believed that undercounting of a group would be more likely than over-counting. The final datasets contained a record for each unique sighting, the number of individuals in the group, distance from the trackline and whether the group was detected by the front and/or rear observer.

Detection Function Analysis

Hector's dolphin abundance was estimated using mark-recapture distance sampling (MRDS) techniques (e.g., Buckland et al. 2004, Borchers et al. 2006, MacKenzie & Clement 2016a, 2016b). The 'symmetric' parameterisation used by MacKenzie and Clement (2016b) is applied

here, which also allows for a lack of independence between the observer detections. A brief summary of the method is given below.

For the purpose of abundance estimation, the key probability to be determined from the data is the probability of detecting a dolphin group (given that it is present) by at least one of the observer positions on the same side of the aircraft. Denote this as $p_{\bullet}(d_i, s_i)$ where d_i and s_i are the distance and group size measured for the ith group respectively. With the double observer setup, there are four possible outcomes in terms of sighting a dolphin group within a survey transect; 1) sighted by both observers; 2) sighted from the front position, but not the rear; 3) sighted from the rear position, but not the front; or 4) sighted by neither observer. These four outcomes are mutually exclusive, and each outcome has an associated probability, the sum of which must equal 1, therefore three of these probabilities can be estimated with the fourth being obtained by subtraction. Note that $p_{\bullet}(d_i, s_i)$ is the sum of the probabilities for the first three outcomes, hence $1 - p_{\bullet}(d_i, s_i)$ is the probability associated with the outcome of a dolphin group not being sighted by either observer.

There are multiple parameterizations that could be used for determining $p_{\bullet}(d_i, s_i)$ (e.g., Laake & Borchers 2004, Buckland et al. 2010, MacKenzie & Clement 2016a) and the one used here is:

$$p_{\bullet}(d_i, s_i) = 1 - \left[1 - p_F(d_i, s_i)\right]\left[1 - p_{R|NF}(d_i, s_i)\right] \qquad \text{(Eqn. 1)}$$

where $p_F(d_i, s_i)$ is the probability of the dolphin group being observed from the front observer position and $p_{R|NF}(d_i, s_i)$ is the probability of the dolphin group being observed from the rear position given it *was not* detected by the front observer (*NF*=not front). Note that using this symmetric parameterisation, Eqn. 1 works out to be equivalent to:

$$p_{\bullet}(d_i, s_i) = 1 - \left[1 - p_R(d_i, s_i)\right]\left[1 - p_{F|NR}(d_i, s_i)\right].$$

The parameterization used here estimates components $p_{F|NR}(d_i, s_i)$, $p_{R|NF}(d_i, s_i)$ and $\upsilon(d_i)$, where $\upsilon(d_i)$ is an odds ratio that determines how the odds of detection changes for an observer position if a group is detected from the other observer position (hence the symmetry). Note that an odds ratio equal to 1 indicates that detections are independent from each observer position. From these components the probability of a dolphin group being detected from the front position given that it was detected from the rear position ($p_{F|R}(d_i, s_i)$) can be calculated as:

$$p_{F|R}(d_i, s_i) = \frac{\upsilon(d_i) p_{F|NR}(d_i, s_i)}{1 - p_{F|NR}(d_i, s_i)[1 - \upsilon(d_i)]},$$

with a similar calculation for $p_{R|F}(d_i, s_i)$. This leads to the unconditional probability of a dolphin group being detected from the front position being calculated as:

$$p_F(d_i, s_i) = \frac{p_{F|NR}(d_i, s_i) p_{F|R}(d_i, s_i)}{p_{F|R}(d_i, s_i)[1 - p_{R|F}(d_i, s_i)] + p_{R|F}(d_i, s_i) p_{F|NR}(d_i, s_i)}.$$

Covariates

The effects of distance, observer, and group size on detection probabilities were considered by fitting a range of models to the collected data. All covariates were included by using the logit-link function, which is equivalent to performing logistic regression. How detection varied with distance was investigated using three different functional forms (on the logit scale); 1) linear; 2) quadratic; and 3) a natural spline with two internal knots. A natural spline is a method for fitting a flexible, non-parametric curve to data. For each functional relationship for distance ($f(d)$), general equations can be expressed for each of $p_{F|NR}(d_i, s_i)$ and $p_{R|NF}(d_i, s_i)$ (Eqns 2 and 3, respectively) from which six models were considered resulting from the application of various constraints across the regression coefficients.

$$\text{logit}\left(p_{F|NR}(d_i, s_i)\right) = \ln\left(\frac{p_{F|NR}(d_i, s_i)}{1 - p_{F|NR}(d_i, s_i)}\right) = a_1 + \boldsymbol{\beta}_1 f(d_i) + c_1 s_i \qquad (2)$$

$$\text{logit}\left(p_{R|NF}(d_i, s_i)\right) = \ln\left(\frac{p_{R|NF}(d_i, s_i)}{1 - p_{R|NF}(d_i, s_i)}\right) = a_2 + \boldsymbol{\beta}_2 f(d_i) + c_2 s_i \qquad (3)$$

The six models were:

1. different intercept terms and different coefficients for *f(d)* for each observer position, i.e., $a_1 \neq a_2$, $\boldsymbol{\beta}_1 \neq \boldsymbol{\beta}_2$ and $c_1 = c_2 = 0$.

2. different intercept terms, but the same coefficients for *f(d)* for each observer position, i.e., $a_1 \neq a_2$, $\boldsymbol{\beta}_1 = \boldsymbol{\beta}_2$ and $c_1 = c_2 = 0$.

3. same intercept and same coefficients for *f(d)* for each observer position, i.e., $a_1 = a_2$, $\boldsymbol{\beta}_1 = \boldsymbol{\beta}_2$ and $c_1 = c_2 = 0$.

4. as model 1, with constant effect of group size for both observer positions, i.e., $a_1 \neq a_2$, $\boldsymbol{\beta}_1 \neq \boldsymbol{\beta}_2$ and $c_1 = c_2$.

5. as model 2, with constant effect of group size for both observer positions, i.e., $a_1 \neq a_2$, $\boldsymbol{\beta}_1 = \boldsymbol{\beta}_2$ and $c_1 = c_2$.

6. as model 3, with constant effect of group size for both observer positions, i.e., $a_1 = a_2$, $\boldsymbol{\beta}_1 = \boldsymbol{\beta}_2$ and $c_1 = c_2$.

Apparent lack of independence between observers (which may be due to response to cues from the other observer, or unmodelled heterogeneity in detection; Laake & Borchers 2004) was incorporated through the odds ratio $\upsilon(d_i)$ which was modelled on the natural log scale. That is,

$$\ln(\upsilon(d_i)) = a_3 + \beta_3 d_i \qquad (4)$$

noting that only a linear effect with distance was considered. MacKenzie & Clement (2016b) considered four models for dependence:

1. full independence, i.e., $a_3 = \beta_3 = 0$ (hence $v_{R/F}(d_i) = 1$).

2. constant dependence at all distances i.e., $a_3 \neq 0$ and $\beta_3 = 0$.

3. dependence between observer position changes linearly with distance, with full independence at the track line, i.e., $a_3 = 0$ and $\beta_3 \neq 0$ (point independence)

4. as for model 3, but dependence between observers at track line is estimated rather than assuming point independence i.e., $a_3 \neq 0$ and $\beta_3 \neq 0$ (limiting independence, Buckland et al., 2010).

The constant dependence and limiting independence models (models 2 and 4 above) did not provide reliable results (i.e., unreasonably large estimates with large standard errors) for the SCSI reanalysis that MacKenzie & Clement (2016b) conducted, presumably due to small sample sizes. Therefore, only the full independence and point independence models were considered here.

While the model has been described above in terms of detection probabilities that are conditional upon the group not being detected from the other observer position, and an odds ratio, this is equivalent to simply using the detection/non-detection of a dolphin group from one observer position, as the basis for a covariate in the detection function for the other observer position (MacKenzie & Clement 2016b). That is, Eqns. 2 or 3 could be combined with Eqn. 4 for a more general expression for the detection probability function. For example, for the front observer position:

$$\mathrm{logit}\left(p_F(d_i, s_i)\right) = a_1 + \beta_1 f(d_i) + c_1 s_i + X_{Ri}\left(a_3 + \beta_3 d_i\right)$$

where X_{Ri} indicates whether the ith group was detected from the rear observer position (=1 if detected, =0 otherwise).

Model Selection and Diagnostics

For each data set, 36 models were considered for the analysis (3 distance relationships $\times$ 6 detection models $\times$ 2 dependence models) and compared using Akaike's Information Criterion (AIC; Burnham & Anderson 2002) to determine the level of evidence for each effect. Goodness-of-fit of the detection function was also assessed using quantile-quantile (q-q) plots along with a Kolmogorov-Smirnov (KS) test and Cramer-von Mises (CvM) test (Buckland et al. 2004).

Model averaging was used to obtain an overall estimate of abundance based upon AIC model weights where there was model selection uncertainty (i.e., models incorporating different factors that have similar levels of support from the data; Anderson 2008). AIC model weights were re-calculated to ensure that the weights for the included models summed to 1.0. Stratum-specific detection functions were not considered as few strata would have sufficient sightings to do so.

2.4 Availability Bias

MacKenzie et al. (2012) emphasised the importance of the availability bias for Hector's dolphins given that it is a fundamentally important component for obtaining a reliable estimate of total abundance. While two different methods were used to assess Hector's dolphin surface availability along the ECSI and WSCI surveys, only helicopter methods were undertaken in SCSI due to low population abundance. As relatively few sightings were expected, the number of opportunities to undertake circlebacks (i.e., the sample size) would be insufficient for reliable estimation of availability.

Helicopter Protocols

Surface availability was estimated using dive/surface intervals of Hector's dolphins collected using a sampling protocol and analysis modified from Slooten et al. (2004) and Clement et al. (2011) and detailed in MacKenzie & Clement (2014). Helicopters searched for dolphins using a similar transect pattern to that used by the fixed-wing airplane; a perpendicular transect was flown out from the shore to approximately 5–10 nmi (depending on location and water depth), the helicopter then travelled parallel to the shore for approximate 1–2 nmi before surveying back towards the shore and maintaining a height of 500 ft. Once a group of dolphins was sighted, the helicopter hovered off to one side or slowly circled the group. While hovering/circling, the observer recorded the duration of the groups' dive and surface intervals, as well as group size and obvious behavioural states, into a continuously running dictaphone for approximately ten minutes or until the group disappeared. A range of group sizes, dive behaviours (synchronous, independent, etc.) and age classes as well as environmental conditions (e.g. Beaufort state, glare and water colour) were observed.

Our analysis included only complete dive cycles (i.e. dropping the first surface and last dive interval as needed) to calculate the average time a group was visible near the surface and the average time below the surface.

From Laake & Borchers (2004), the probability of a group being available (P_α) can be calculated from dive cycle data by:

$$P_\alpha = 1 - \frac{\bar{b}\exp(-t/\bar{b})}{\bar{u} + \bar{b}}$$
(5)

where $\bar{b}$ is the average time below the surface, $\bar{u}$ the average time up or near the surface and t is the time frame for which the group is within the view of the observers from the aircraft. The standard error for P_α can be calculated as:

$$SE(P_\alpha) = \sqrt{\left[\frac{\bar{b}\exp(t/\bar{b})}{(\bar{u}+\bar{b})^2}\right]^2 V_{\bar{u}} - 2\bar{u}\bar{b}\left[1 + \frac{t(\bar{u}+\bar{b})}{\bar{u}\bar{b}}\right]V_{\bar{u}\bar{b}} + \bar{u}^2\left[1 + \frac{t(\bar{u}+\bar{b})}{\bar{u}\bar{b}}\right]^2 V_{\bar{b}}}$$
(6)

where $V_{\bar{u}}$ and $V_{\bar{b}}$ are the variances for $\bar{u}$ and $\bar{b}$ respectively, and $V_{\bar{u}\bar{b}}$ is the covariance for the two means.

Only the Te Waewae Bay strata were sampled, as the low number of survey sightings elsewhere did not justify the longer search times needed to collect sufficient dive profile sample sizes. The value from the Te Waewae Bay strata was applied to all other strata.

2.5   Abundance Estimation

The number of dolphins within the area of stratum k covered by the surveys is estimated using a Horvitz-Thomson type estimator, i.e.,

$$\hat{N}_{ck} = \sum_{i=1}^{n_k} \frac{s_i}{E(p(s_i))} \qquad (8)$$

where n_k is the number of groups detected in the stratum, s_i is the size of the ith group and $E(p_\bullet(s_i))$ is the expected probability of the ith group being detected given its size, which is obtained from the detection function analysis.

The number of *available* dolphins (i.e., near the surface with a non-zero change of detection by the observers in the plane) within the stratum is therefore

$$\hat{N}_{ak} = \frac{A_k \hat{N}_{ck}}{a_k} \qquad (9)$$

where, A_k is the total area of the stratum; $a_k = 2wL_k$ is the area covered by the survey transects with w being the truncated width (0.26 km) and L_k the total transect length flown. Note that this calculation is valid even when a stratum has been surveyed multiple times. Accounting for availability, the total number of dolphins within a stratum is therefore:

$$\hat{N}_k = \frac{\hat{N}_{ak}}{\hat{P}_{ak}} \qquad (10)$$

with total abundance being:

$$\hat{N} = \sum_{k=1}^{K} \hat{N}_k \qquad (11)$$

Details on the calculation of the standard errors are given in MacKenzie & Clement (2014) but note that they are extensions of the methods used by Buckland et al. (2010). It should also be noted that given that some strata share parameters (either through the detection function or availability estimates), the standard errors from the stratum-specific abundance estimates cannot be simply combined to obtain the standard error for total dolphin abundance.

As there may be model selection uncertainty associated with the detection function analysis, which would lead to different estimates of abundance, AIC-based model averaging was used to combine the abundance estimates resulting from each detection function model (Burnham & Anderson, 2002; Anderson 2008, see supplemental materials in MacKenzie & Clement 2016c). Note that by using these calculations, variation in the different abundance estimates is incorporated into the standard error of the final estimate. Based upon an averaged estimate of abundance ($\hat{N}$) and its associated standard error (*SE*), the lower and upper limits of a Wald-lognormal 95% confidence interval were calculated.

2.6   Distribution Analyses

Density surface modelling (DSM; Buckland et al. 2004) was used to examine Hector's dolphin distribution, where distribution is defined as those areas with a non-negligible predicted

density. DSM techniques combine the survey data with a spatial analysis to model how density at the time of surveying varies across a region according to spatially defined environmental variables (e.g. distance from shore) while taking into account the probability of detecting the animals (Gomez de Segura et al. 2007). Further corrections can be made to account for dolphin availability. It is important to note that a DSM produces a predicted density surface based upon line-transect data collected during the survey. Spatial and habitat information is used to explain variability in where dolphins were sighted at the time of the survey, which results in the prediction surface. The estimated prediction surface may be sensitive to the exact location of the sightings with an alternative data set leading to a different prediction surface. Even though a DSM may use habitat variables, it is not a study of habitat preferences of the animals. The results cannot be used to make broad conclusions about the habitat preference of Hector's dolphins.

DSM protocols

The DSM was developed by using the top-ranked detection function model from the full distance sampling data set. Easting, northing and distance from shore were included as covariates for the DSM. The analyses were undertaken within the statistical software R using a combination of custom code and the package *dsm* (v.2.2.16). Transect lines were divided into segments approximately 1 km long and 0.520 km wide, with the easting and northing coordinates for the centre point of the segment determined. Values for easting, northing and distance from shore were obtained from a prediction grid with 5×5 km cells. Dolphin abundance was estimated for each transect segment based upon the number of dolphins sighted in each segment, the estimated detection function and helicopter-based estimates of regional availability (Buckland et al. 2004). That is:

$$\hat{N}_i = \sum_{j=1}^{n_i} \frac{s_{ij}}{E\left(p_\bullet\left(s_{ij}\right)\right)\hat{P}_{\alpha k}}$$

where $\hat{N}_i$ is the estimated abundance for segment i, n_i is the number of groups in the segment, s_{ij} is the size of the jth group in the segment, $E\left(p_\bullet\left(s_{ij}\right)\right)$ is the expected probability of detecting a group of size s_{ij}, and $\hat{P}_{\alpha k}$ is the estimated availability probability for stratum k (which segment i is contained within).

A generalised additive model (GAM) was used to model the segment-specific abundance estimates based on the above covariates (with easting and northing entered as a bivariate spline term). The results of the GAM were used to predict dolphin density across the study region using the prediction grid that was defined at a scale of 5×5 km cells.

Standard errors were obtained using a parametric bootstrap to accommodate uncertainty in both the detection function and DSM. It was implemented in the following steps:
1. Fit the detection function and DSM to the observed data to estimate the number of individual dolphins.
2. Refit DSM to estimate the density of available dolphin groups (as sightings are made of groups not individuals).
3. Generate locations of available (e.g., near surface) groups using a random Poisson point process where the process intensity is obtained from the adjusted group-level DSM fitted in step 2.

4. Determine perpendicular distance of the group from nearest transect line. Retain groups that are within the area covered by the survey (i.e., within 0.26 km). Other groups are not retained as they have no chance of being sighted.
5. Randomly generate group size using a group-size frequency table. This table is based on the observed group frequency, with correction for detection probability being different for different group sizes. That is, $\hat{f}_s = \dfrac{n_s / E[p_\bullet(s)]}{\hat{N}_{gc}}$, where $\hat{f}_s$ is the estimated frequency of group size s, n_s is the number of observed groups of size s, $E(p_\bullet(s))$ is the expected probability of detecting a group of size s within the covered area and $\hat{N}_{gc}$ is the estimated number of groups within the covered area
6. Using the detection function estimated in step 1, determine the probability of each group being detected from either observer position, both observer positions, or not detected, given its distance from the line and size. This defines the probability of each of the four mutually-exclusive observation outcomes.
7. Generate a multinomial random variable to simulate the observation outcome for whether a group was sighted from each observer position.
8. Using the groups sighted at least once, refit the detection function model used in step 1 to obtain detection estimates pertinent to the generated (i.e., bootstrapped) data set.
9. For each region, generate a new availability estimate by drawing a random value from a logit-normal distribution with mean and standard deviation equal to the logit-transformed regional availability estimate and associated standard error.
10. Using the detection function model fit in step 8, and availability estimates obtained in step 9, refit the DSM used in step 1 to obtain a predicted density surface (of individuals) for the bootstrap data set.
11. Repeat steps 3–10 a sufficiently large number of times. The standard deviation of summaries calculated from the bootstrapped DSMs can be used to approximate the standard errors of the corresponding quantities from the DSM for the real data.

MacKenzie et al. (2012) noted from simulation studies that resulting maps from a DSM analysis were sensitive to the exact location of detections when using a 5 × 5 km prediction grid and recommended that for the purpose of robust inferences about distribution, coarser spatial scales (e.g., cells of hundreds of square kilometres) should be used. While the results of the DSM are presented at the prediction grid scale, extreme caution is advised in terms of using the DSM to make such fine scale inferences because the maps will be sensitive to where dolphins were observed at the time of the survey. Changes in where dolphins were sighted, either due to dolphin movement or random chance, may lead to quite different maps. Hence, the DSM results may not accurately represent distribution information over a longer timeframe. It is recommended that the results from the prediction grid that have been aggregated to the courser scale of the strata be used for distribution and abundance inferences. A grid cell was defined to be associated with a defined stratum if its centroid was within the stratum boundaries, therefore given the resolution of the prediction grid, stratum areas are slightly different compared to those used previously.

Maps of the DSM results are expressed as relative densities. That is, the estimated density for a grid cell or stratum relative to the overall density;

$$\frac{\hat{N}_k / A_k}{\hat{N} / A},$$

as a means to identify areas of relative higher or lower density that are robust to the magnitude of absolute abundance estimates. Values over 1 indicate areas with densities that are greater than the overall average. Note that the relative density can also be interpreted as the fraction of the total population in cell or stratum k, relative to the proportion of the total area contained within that cell or stratum, i.e.,

$$\frac{\hat{N}_k / \hat{N}}{A_k / A}.$$

3. RESULTS

3.1 SCSI Abundance Models

A summary of the summer sighting data is given in Table 4 and Sections A and B of the Supplemental Material (SM). These sample sizes are within the recommended minimum of 60–80 sightings for estimating abundance (Buckland et al. 2001). For the front observer position during the summer survey, 3 sightings were left truncated (i.e., had distances less than 0.040 km) and 1 sighting was right truncated (distance more than 0.300 km). For the rear observer position, 1 sighting was left truncated, which was also truncated for the front observer position, and 1 sighting was right truncated.

Table 4: Summary of the sighting data from the SCSI aerial surveys. 'Verified' indicates the numbers post-verification; 'Full' indicates the numbers used in the analysis where sightings were left truncated at 0.040 km and right truncated at 0.300 km for both observer positions. Note that the number of groups sighted from both positions are also included in the front and rear totals.

	Verified	Full
Total Sightings	80	75
Total Front	55	51
Total Rear	54	52
Both (duplicates)	29	28
Individuals		154
Average Group Size		2.05
SD Group Size		1.74
Range Group Size		1–12
Transect Length (km)		**2574**

Detection function analysis

The top 10 models (as ranked by AIC) for the full data set are given in Table 5. The results exhibit a high degree of model selection uncertainty with all of the models having relatively low AIC model weights, therefore the top ten models were used to produce model averaged estimates of abundance after adjusting their AIC model weights such that they sum to 1. Seven of the top ten models assume a linear relationship with distance (and two quadratic-based models and one spline), four include an overall observer position effect and only two of the top ten models allow the detection function parameters to be different from each observer position. Nine of the models include a group-size effect and six have point independence. Overall, models with a linear distance relationship, no observer effects and a group-size effect have the most support. ESW estimates are similar to previous results for SCSI from comparable models (MacKenzie & Clement 2016b).

Plots of the fitted detection functions and empirical histograms of detection rates do not indicate any systematic concerns about lack of fit for any of the top ten models, particularly for $p_{\bullet}(d_i, s_i)$, which is the most relevant in terms of estimating abundance. The fitted detection functions for the top ranked models are presented in Section C of the SM for illustration along with the q-q plots. The q-q plots (SM Section C) and goodness of fit tests (Table 6) do not indicate any evidence of lack of fit for the top ten models.

Table 5: Top 10 AIC-ranked models for the detection function analysis for sightings between 0.04 and 0.30 km from the transect line in the summer. Model components identify the structure of the detection function model; $f(d)$ **is the functional relationship with distance on the logit scale (L=linear, Q=quadratic, S=Spline), Obs indicates whether the intercept term is different for each observer position (Y=Yes, N=No),** $\beta_1 \neq \beta_2$ **indicates whether the regression coefficients for the effect of distance on detection is different for each observer position (Y= Yes, N= No), Size indicates whether group size has an effect on detection (Y=Yes, N=No) and Dep. indicates the form of dependence in detection between observer positions (FI=Full Independence and P = Point). ΔAIC is the relative difference in AIC values, wgt is the AIC model weight, wgt* is the adjusted AIC weight for the models used for inference, -2***l*** is twice the negative log-likelihood, pars. is the number of parameters in the model,** $\hat{N}_{cg}$ **is the estimated number of dolphin groups in the covered area,** $SE(\hat{N}_{cg})$ **is the standard error for** $\hat{N}_{cg}$**, and ESW is the effective strip width accounting for detection and perception bias.**

					Model Components							
$f(d)$	Obs	$\beta_1 \neq \beta_2$	Size	Dep.	ΔAIC	wgt	wgt*	-2*l*	pars.	$\hat{N}_{cg}$	$SE(\hat{N}_{cg})$	ESW
L	N	N	Y	P	0.00	0.22	0.27	130.65	4	165	28	0.118
L	N	N	Y	FI	0.68	0.15	0.19	133.33	3	144	19	0.135
Q	N	N	Y	P	1.81	0.09	0.11	130.47	5	168	29	0.116
L	Y	N	Y	P	1.98	0.08	0.10	130.63	5	165	28	0.118
Q	N	N	Y	FI	2.65	0.06	0.07	133.30	4	143	20	0.136
L	Y	N	Y	FI	2.66	0.06	0.07	133.31	4	144	19	0.136
L	Y	Y	Y	P	2.89	0.05	0.06	129.54	6	165	28	0.118
L	N	N	N	P	3.52	0.04	0.05	136.17	3	161	28	0.121
S	N	N	Y	P	3.71	0.03	0.04	130.36	6	168	30	0.116
L	Y	Y	Y	FI	3.73	0.03	0.04	132.39	5	144	19	0.136

Table 6: Goodness of fit tests for top ten ranked models for the detection function analysis of the full summer data set. Given are the Cramer-von Mises (CvM) and Kolmogorov-Smirnov (KS) tests with associated p-values.

Model Rank	CvM	p-value	KS	p-value
1	0.099	0.591	0.089	0.587
2	0.174	0.323	0.121	0.219
3	0.092	0.626	0.075	0.789
4	0.099	0.591	0.089	0.587
5	0.185	0.300	0.126	0.183
6	0.174	0.323	0.121	0.219
7	0.098	0.597	0.088	0.607
8	0.096	0.604	0.095	0.514
9	0.090	0.634	0.075	0.787
10	0.175	0.323	0.121	0.222

Availability Bias

Helicopter Dive Profiles

During the survey, dive information was collected on 32 different dolphin groups equating to over 650 complete dive cycles within Te Waewae Bay region only, of these 28 groups were suitable for further analysis (Table 7; Figure 3). This effort is similar to regional sampling levels from both the ECSI and WCSI surveys; ranging from 12 to 22 groups and 24 to 192 dive cycles, and 19 to 22 groups and 340 to 356 dive cycles, respectively. In the ECSI survey (MacKenzie & Clement 2014), it was determined that fixed objects are within an observer's view for about six seconds on average, hence $t=6$ has been used to correct for availability bias when estimating abundance (Table 7).

Table 7: Summary of dive-cycle data and availability estimates. Estimates presented are the number of groups data were collected on (n), average time on or near the surface ($\bar{u}$), average dive time ($\bar{b}$), variance for the average surface time ($V_{\bar{u}}$), variance for the average dive time ($V_{\bar{b}}$) and covariance between average surface and dive time ($V_{\bar{u}\bar{b}}$). All times are given in seconds. Estimated probability of a group being available ($\hat{P}_\alpha$) for $t = 6$ seconds and associated standard error (SE).

Area	n	$\bar{u}$	$\bar{b}$	$V_{\bar{u}}$	$V_{\bar{b}}$	$V_{\bar{u}\bar{b}}$	$\hat{P}_\alpha$	SE
Te Waewae Bay	28	21.1	22.4	12.2	9.6	4.8	0.61	0.07
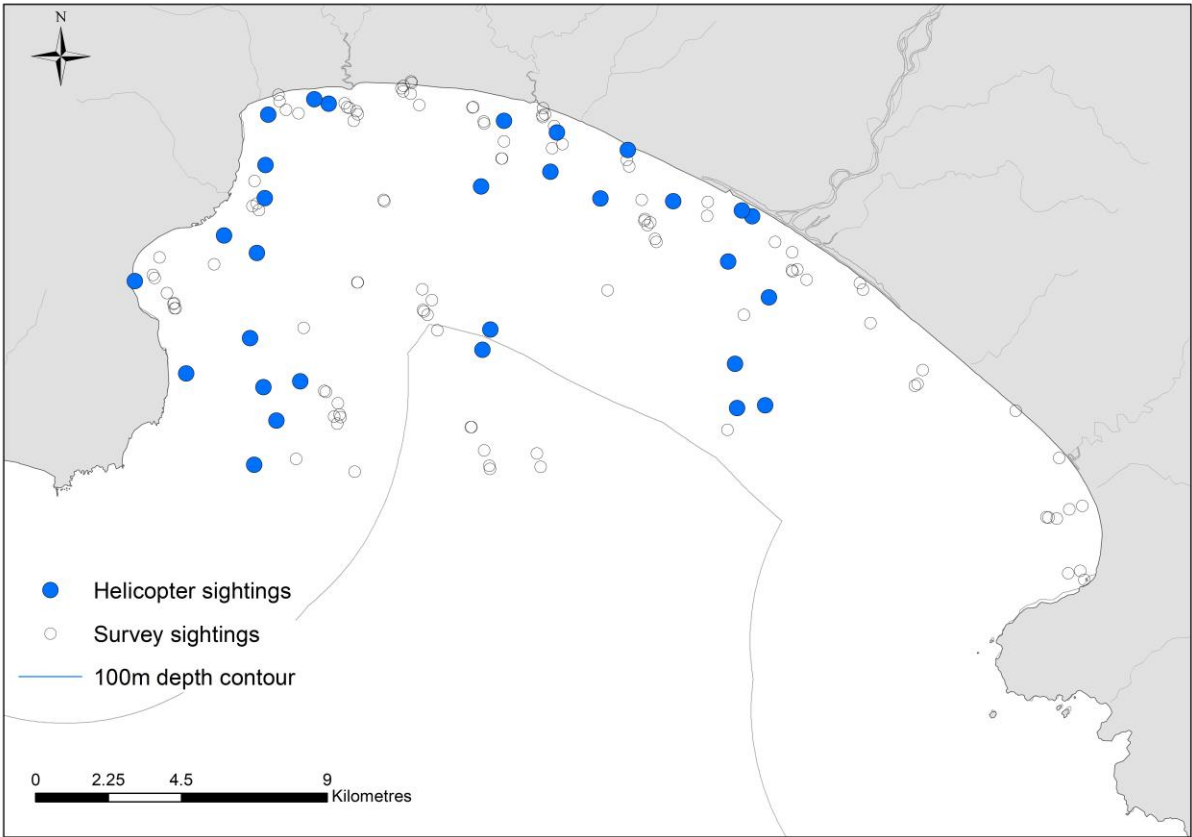
Figure 3: Availability sighting locations from helicopter observations (blue dots) within Te Waewae Bay relative to the locations of survey sightings (open dots).

SCSI Abundance Estimates

Summer estimates of dolphin abundance, after correcting for availability and perception bias, are given in (Table 8). Details of the stratum-specific estimates from each detection function are given in the SM (Section D). These results provide an estimate of Hector's dolphin summer abundance along the SCSI survey area of 332 (CV: 22%; 95% CI: 217–508).

Table 8: Model averaged summer abundance estimates and standard errors for each stratum from sightings between 0.04–0.30 km. Given are the estimated abundance of Hector's dolphins (corrected for availability bias; $\hat{N}_k$ using the availability estimates from the dive-cycle data), associated standard error and lower and upper limits of a 95% confidence interval.

Coastal Section	Offshore Stratum (nmi)	$\hat{N}_k$	SE	Lower	Upper
Te Waewae Bay	0 – 4	302	70	193	471
	4 – 12	30	12	15	63
Toetoes	0 – 4				
Elsewhere	0 – 4				
	4 – 20				
Total		**332**	**73**	**217**	**508**

3.2   SCSI Distribution Results

Hector's dolphins along the south coast were generally found quite close to shore (i.e. within 2 nmi) and in relatively shallow depths (e.g. less than 30 m; Table 9, Figure 4). The furthest survey sighting from shore was approximately 10.2 km (6.3 nmi), while still confined with the Te Waewae Bay region. The 2010 survey, whose main objective was to document dolphin distribution, had two summer sightings further offshore of Curio/Porpoise Bay, the furthest being 17.8 km (9.6 nmi). All other previous boat-based surveys and MPI observer sightings have also been close to the shore (Figure 5). As no sightings occurred within the 12–20 nmi stratum, the survey is likely to have encompassed the full offshore limits of this population.

The replicate surveys with the Te Waewae Bay strata also demonstrate the variability present between dolphin numbers (i.e. 16 to 59 animals) and locations across several days and even within the same day (Figure 6). In general, more sightings were observed in later surveys and there was a perceivable shift towards the eastern side of the bay.

Table 9: The mean and maximum distance from shore (km) and depths (m) at which summer and winter survey sightings of Hector's dolphin occurred.

Stratum	Distance offshore (km)		Depth (m)	
	Mean	Max	Mean	Max
Te Waewae Bay	2.3	10.2	9.3	24.0
Toetoes	1.5	NA	20.0	NA
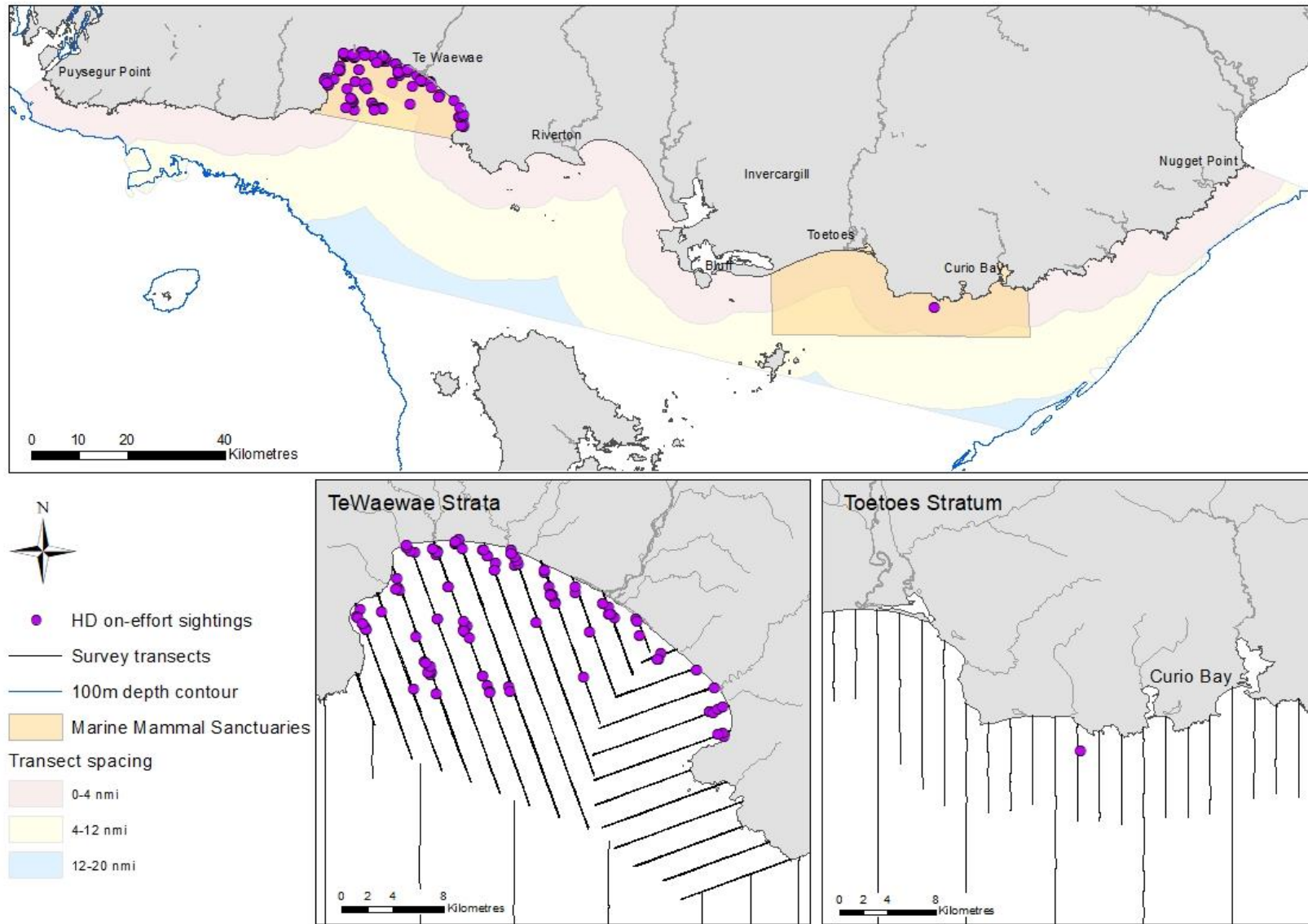
Figure 4: Hector's dolphin summer distribution from aerial line-transect surveys of SCSI. Insets represent Te Waewae Bay (left) and Toetoes/Curio Bay (right).
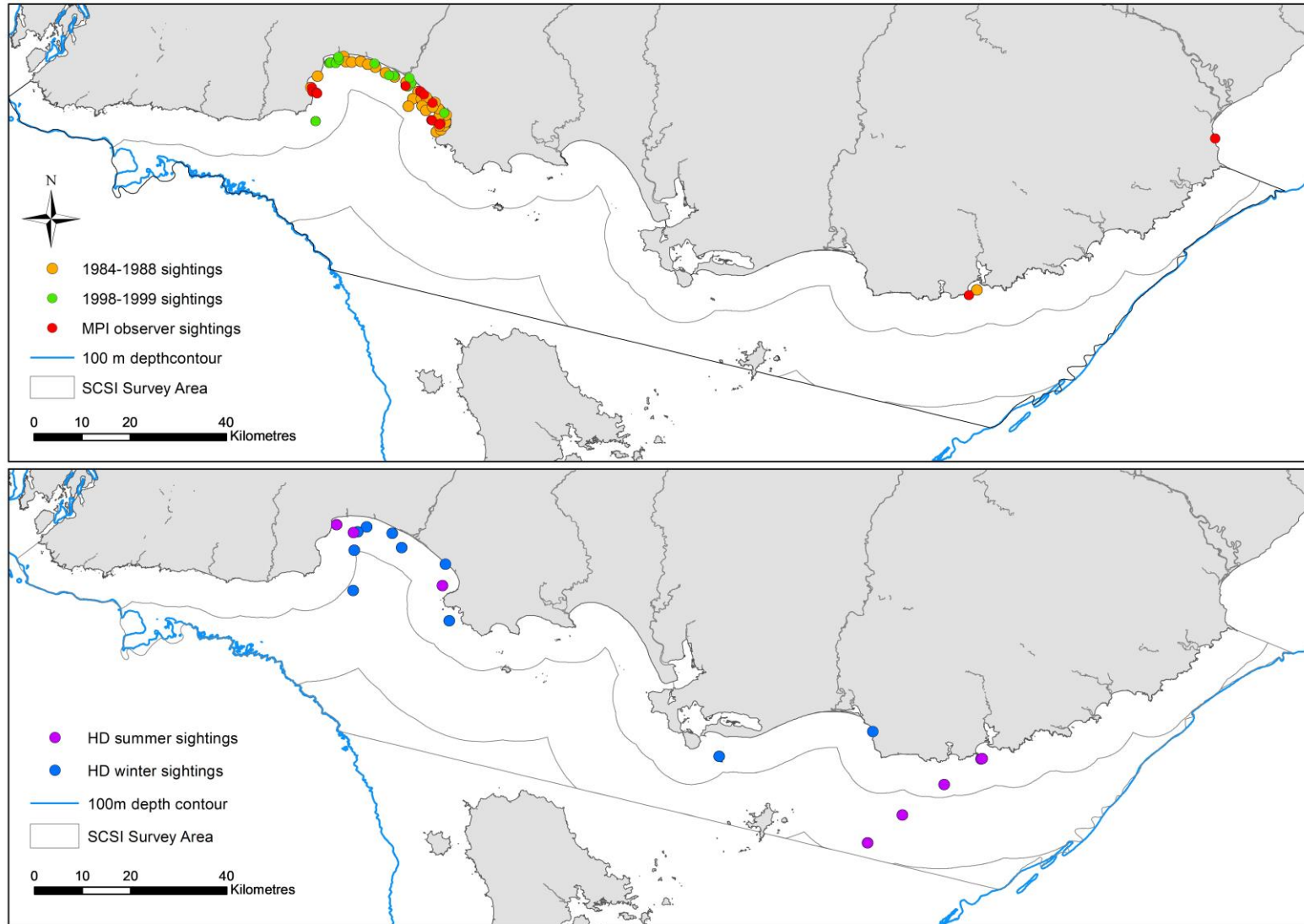
Figure 5: Locations of Hector's dolphin sightings along the SCSI from previous boat-based surveys and Fisheries New Zealand observers (top) and the 2010 aerial survey (bottom).
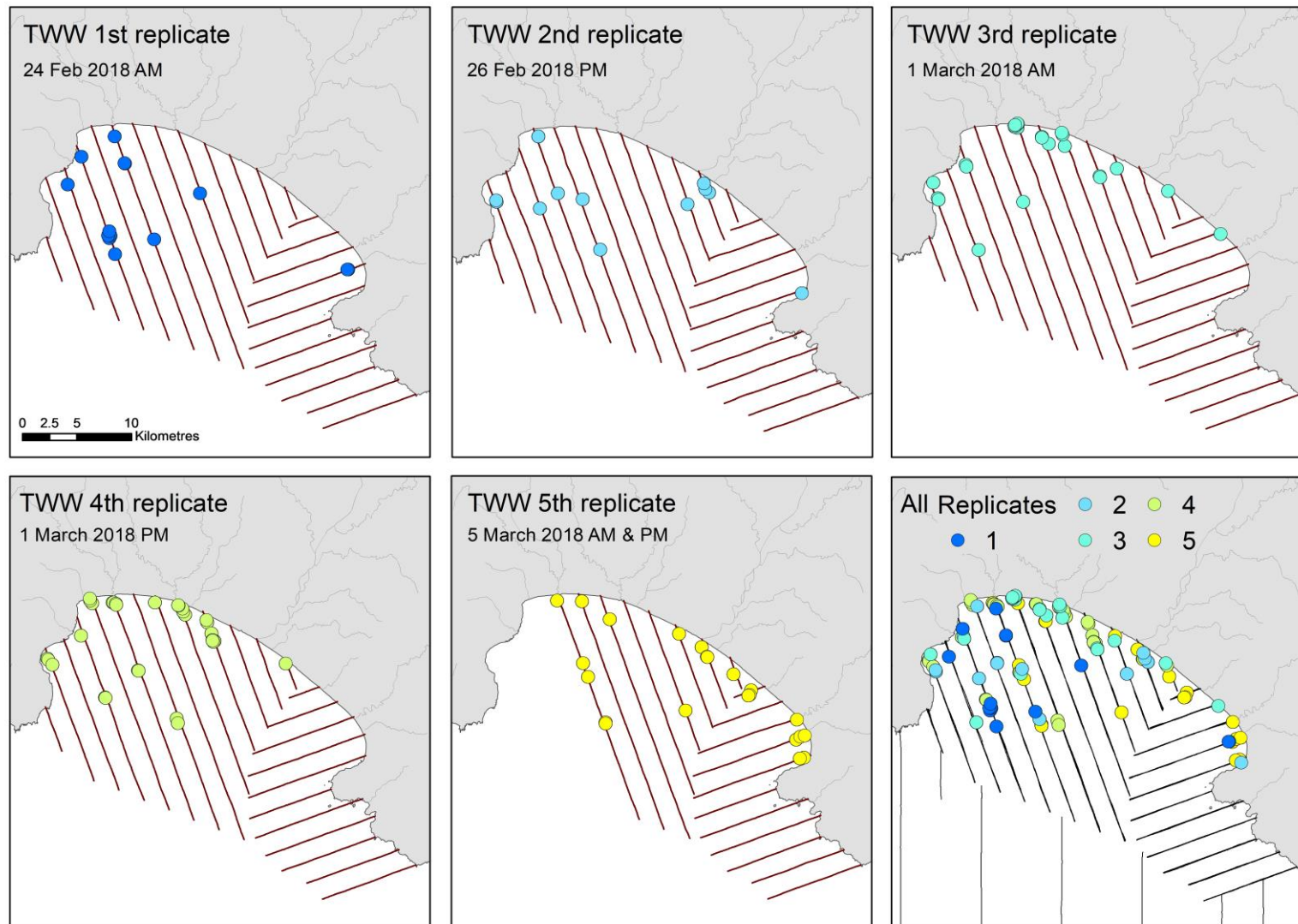
Figure 6: The locations of Hector's dolphin sightings within the Te Waewae Bay strata listed in order of replicate survey from the top left corner to the bottom right corner. Final image displays all replicate surveys together.

The results of the summer DSMs are given in Figure 7. Table 10 lists the group-size frequencies used in the parametric bootstrap. Standard errors were obtained using 510 bootstrap data sets. This is a sufficient number for approximating standard errors (Manly 1997). Valid standard errors for the detection function were not obtained for five bootstrap datasets for the analysis. Therefore, standard errors for the summer DSM were determined from 505 bootstrap samples.

Total abundance was estimated from the DSM as 315 (SE = 88). The value is in good general agreement with the non-DSM abundance estimate using the top-ranked detection function model and the helicopter-based estimates of availability (345, SE = 71, Table SM.D.1). The right-hand panels of Figure 7 indicate the precision of the relative abundance estimates from the DSM and tend to be greatest in those areas with higher relative density.

Table 10: Group-size frequency table used to randomly generate group sizes in the parametric bootstrap procedure. Results presented are the number of observed groups of size s (n_s), the expected probability of detecting a group of size s within the covered area ($E(p_\bullet(s))$), and the estimated frequency of group size s ($\hat{f}_s$). The estimated number of groups in the covered area ($\hat{N}_{gc}$) was 165.

Size	n_s	$E(p_\bullet(s))$	$\hat{f}_s$
1	38	0.400	0.576
2	20	0.471	0.258
3	7	0.544	0.078
4	5	0.617	0.049
5	2	0.688	0.018
6	1	0.755	0.008
7	1	0.816	0.007
12	1	0.979	0.006
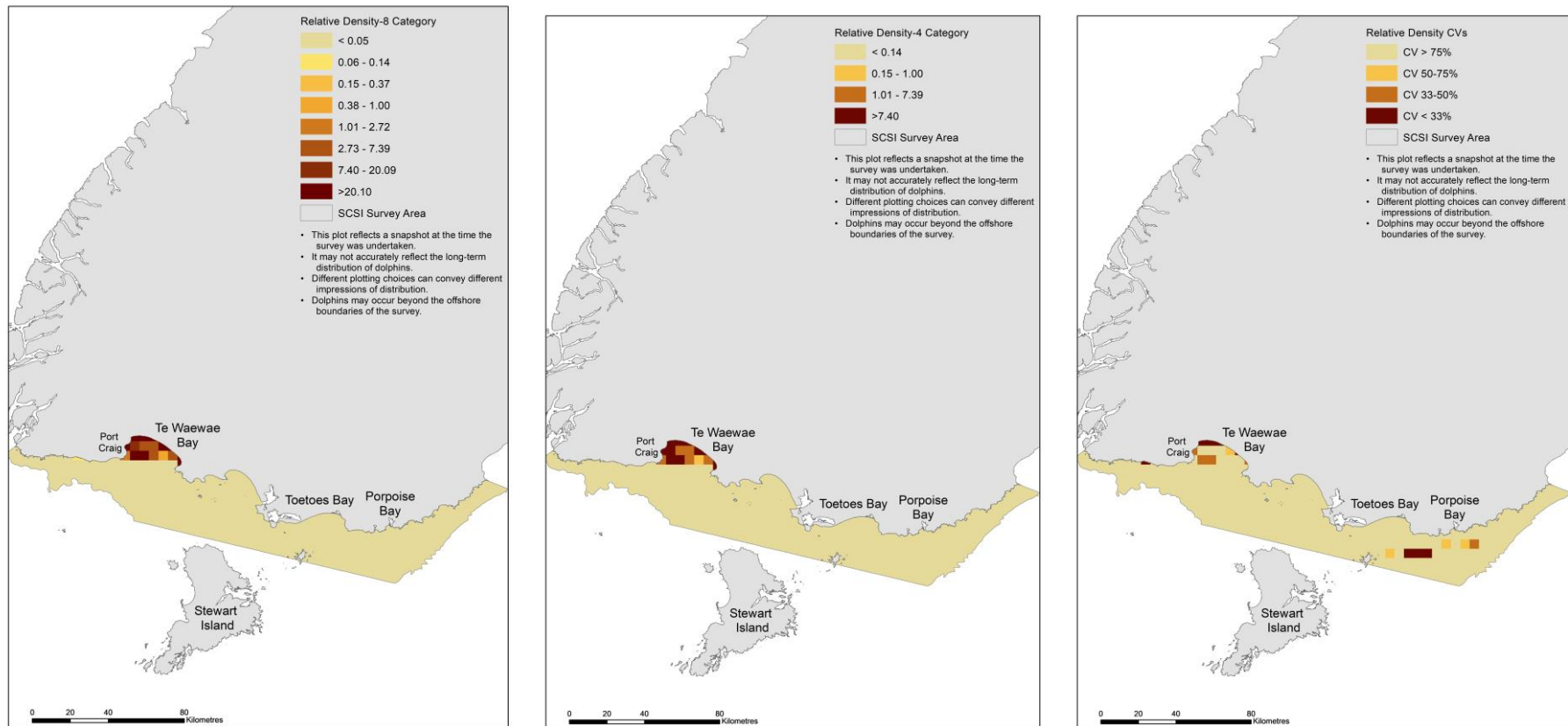
Figure 7: Hector's dolphin summer distribution assessed from aerial line-transect surveys. Panels represent the relative density of Hector's dolphins within 5 km × 5 km grid cells generated from the Density Surface Models with eight categories (left), from the Density Surface Models with four categories (middle), and the precision of estimated relative density with darker colours indicating greater precision; i.e. smaller CVs (right). Relative densities greater than 1 indicate areas with density greater than the overall average density.

4. DISCUSSION

MacKenzie and Clement (2016b, 2016c) reanalysed the aerial survey data of Clement et al. (2010) using the same techniques as those applied here. They estimated Hector's dolphin abundance for the same survey area along the SCSI as 177 for March 2010 (CV: 37%; 95% CI: 88–358), 299 for August 2010 (CV: 47%; 95% CI: 125–714), and a combined estimate of 238 (CV: 40%; 95% CI: 113–503). Our current SCSI estimate (332, CV: 22%; 95% CI 217-508) is in good agreement with these previous estimates.

The availability estimate of Clement et al (2011) was also reanalysed to allow for the length of time a dolphin group would be in an observer's field of view form the aircraft (t=6 seconds) rather than instantaneous availability (i.e. t=0 seconds) used by previous surveys (e.g. Slooten et al 2004, DuFresne & Mattlin 2009). Our current estimate of availability (0.61) was also similar to these reanalysed estimates of 0.57 for March and 0.67 for August.

Hence, the improvement in the precision of the current estimate is likely to be based on sighting an adequate number of groups during the survey (i.e. minimum of 60 sightings) as recommended in the pre-survey simulation report (MacKenzie & Clement 2017). This sighting level was achieved by stratifying the survey area and scaling up effort in Te Waewae Bay, a higher density area for Hector's dolphins, rather than using the distribution approach that was the goal of Clement et al. (2011).

All of the on-effort sightings within 300 m of the transect line were made in the Te Waewae Bay strata. Abundance estimates have not been given for the other areas due to no qualifying sightings, although we stress that the lack of an estimate should not be interpreted indicating that Hector's dolphin is entirely absent from those strata. We strongly suspect that there are Hector's dolphin in those strata, but at such low density that our survey effort was insufficient to detect them. Indeed, there was one on-effort sighting of Hector's dolphin in the Toetoes Bay strata, but it was too far from the transect line to be included in the analysis (360 m).

The alongshore distribution of dolphin density largely matched our *a priori* expectations; based on distribution patterns from previous Hector's dolphin boat and aerial survey work (i.e. Clement et al. 2011, Dawson et al. 2004, Dawson & Slooten 1988). It was anticipated that the greatest densities would be within Te Waewae Bay, which is why the repeated surveys were conducted there. We had expected to sight more dolphin groups in the Toetoes Bay strata than the single sighting of a group. There are regular sightings of Hector's dolphin along many sections of SCSI where none were detected during the aerial surveys, which reinforces that the distribution maps obtained from the DSM are only representative of the distribution at the time of the survey and may not hold more generally.

5. ACKNOWLEDGMENTS

6. REFERENCES

Anderson, D.R. (2008). Model based inference in the life sciences. Springer. New York, USA.

Baker, C.S.; Chilvers, B.L.; Constantine, R.; DuFresne, S.; Mattlin, R.H.; van Helden, A.; Hitchmough, R. (2010). Conservation status of New Zealand marine mammals (suborders Cetacea and Pinnipedia), 2009. *New Zealand Journal of Marine and Freshwater Research, 44(2)*: 101 – 115.

Borchers, D.L.; Laake, J.L.; Southwell, C.; Paxton, C.G.M. (2006). Accommodating unmodeled heterogeneity in double-observer distance sampling surveys. *Biometrics* 62, 372–378.

Buckland, S.T.; Anderson, D.R.; Burnham, K.P.; Laake, J.L.; Borchers, D.L.; Thomas, L. (2001). Introduction to Distance Sampling: Estimating abundance of biological populations. Oxford University Press, New York.

Buckland, S.T.; Anderson, D.R.; Burnham, K.P.; Laake, J.L.; Borchers, D.L.; Thomas, L. (2004). Advanced Distance Sampling: Estimating abundance of biological populations. Oxford University Press, New York.

Buckland, S.T.; Laake, J.L.; Borchers, D.L. (2010). Double-observer line transect methods: levels of independence. *Biometrics* 66: 169–177.

Burnham, K.P.; Anderson, D.R. (2002). Model selection and multimodel inference. 2nd Ed., Springer-Verlag, New York, USA.

Clement, D.; Mattlin, R.; Torres, L. (2011). Abundance, distribution and productivity of Hector's (and Maui's) dolphins Final Research Report, PRO2009-01A. (Unpublished report held by Fisheries New Zealand, Wellington.)

Dawson, S.; Slooten, E. (1988). Hector's Dolphin *Cephalorhynchus hectori*: Distribution and abundance. *Reports International Whaling Commission Special issue 9*: 315–324.

Dawson, S.; Slooten, E.; Du Fresne, S.; Wade, P.; Clement, D. (2004). Small-boat surveys for coastal dolphins: line-transect surveys for Hector's dolphin (*Cephalorhynchus hectori*). *Fishery Bulletin* 102(3): 441–451.

Dawson, S.; Wade, P.; Slooten, E.; Barlow, J. (2008). Design and field methods for sighting surveys of cetaceans in coastal and riverine habitats. *Mammal Review* 38(1): 19–49.

Department of Conservation, Ministry of Fisheries (2007). Hector's and Maui's dolphin threat management plan draft for public consultation. 5 March 2009.http://www.fish.govt.nz/NR/rdonlyres/2088EFD2008C-E2207-4798-9315-C2000AF2002FC2006FFB2002/2000/DRAFTTMPFINAL.pdf

DuFresne, S.; Mattlin, R. (2009). Distribution and Abundance of Hector's Dolphin (Cephalorhynchus hectori) in Clifford and Cloudy Bays (Final report for NIWA project CBF07401). Marine Wildlife Research Ltd.

DuFresne, S.; Mattlin, R.; Clement, D. (2010). Distribution and Abundance of Hector's Dolphin (*Cephalorhynchus hectori hectori*) and Observations of Other Cetaceans in Pegasus Bay. Final Report to the Marlborough Mussel Company, Baseline Monitoring for Environment Canterbury Consent CRC21013A.

Gomez-de-Segura, A.; Hammond, P.S.; Canadas, A.; Raga J.A. (2007). Comparing cetacean abundance estimates derived from spatial models and design-based line transect methods. *Marine Ecology Progress Series* 329: 289–299.

Hamner, R.M.; Oremus, M.; Stanley, M.; Brown, P.; Constantine, R.; Baker, C.S. (2012). Estimating the abundance and effective population size of Maui's dolphins using microsatellite genotypes in 2010–11, with retrospective matching to 2001–07. Department of Conservation, Auckland. 44 p.

Laake, J.L.; Borchers, D.L. (2004). Methods for incomplete detection at distance zero. Pp. 108–189 in *Advanced Distance Sampling*, eds Buckland, S.T.; Anderson, D.R.; Burnham, K.P.; Laake, J.L.; Borchers, D.L.; Thomas, L. Oxford University Press, Oxford.

MacKenzie, D.I.; Clement, D.M. (2014). Abundance and distribution of ECSI Hector's dolphin. *New Zealand Aquatic Environment and Biodiversity Report No. 123*. 79 p.

MacKenzie, D.I.; Clement, D.M. (2016a). Accounting for Lack of Independence and Partial Overlap of Observation Zones in Line-Transect Mark-recapture Distance Sampling. *Journal of Agricultural, Biological, and Environmental Statistics 21:* 41–57. DOI 10.1007/s13253-015-0234-1.

MacKenzie, D.I.; Clement, D.M. (2016b). Abundance and distribution of WCSI Hector's dolphin. *New Zealand Aquatic Environment and Biodiversity Report No. 168*. 67 p.

MacKenzie, D.I.; Clement, D.M. (2016c). Abundance and distribution of WCSI Hector's dolphin. *New Zealand Aquatic Environment and Biodiversity Report No. 168* Supplemental Material 112 p.

MacKenzie D.; Clement, D. (2017). PRO2016-09 Abundance and distribution of Hector's dolphin on South Coast South Island: Pre-survey simulation study: Prepared for MPI. Cawthron Report, No. 3097. 20 p. plus appendix.

MacKenzie, D.I.; Clement, D.; Mattlin, R. (2012). Abundance, distribution and productivity of Hector's (and Maui's) dolphins (Final Research Report, PRO2009-01B). (Unpublished report held by Fisheries New Zealand.)

Manly, B.F.J. (1997). Randomization, bootstrap and Monte Carlo methods in biology. 2nd edition. Chapman and Hall, London, U.K.

Pichler, F.B.; Dawson, S.M.; Slooten, E.; Baker, C.S. (1998). Geographic isolation of Hector's dolphin populations described by mito-chondrial DNA sequences. *Conservation Biology 12*:676–682.

Rayment, W.; Dawson, S.; Slooten, E. (2010a). Seasonal changes in distribution of Hector's dolphin at Banks Peninsula, New Zealand: implications for protected area design. *Aquatic Conservation: Marine and Freshwater Ecosystems 20*: 106–116.

Rayment, W.; Clement, D.; Dawson, S.; Slooten, E.; Secchi, E. (2010b). Distribution of Hector's dolphin (*Cephalorhynchus hectori*) off the west coast, South Island, New Zealand, with implications for the management of bycatch. *Marine Mammal Science 27*: 398−420.

Reeves, R.R.; Dawson, S.M.; Jefferson, T.A.; Karczmarski, L.; Laidre, K.; O'Corry-Crowe, G.; Rojas-Bracho, L.; Secchi, E.R.; Slooten, E.; Smith, B.D.; Wang, J.Y.; Zhou, K. (2008). *Cephalorhynchus hectori maui*. In: IUCN 2011. IUCN Red List of Threatened Species. Version 2011.1.http://www.iucnredlist.org

Slooten, E.; Dawson, S.; Rayment, W. (2004). Aerial surveys for Hector's dolphins: abundance of Hector's dolphins off the South Island west coast, New Zealand. Marine Mammal Science 20, 477–490.

7. Appendices

SECTION A: Summary of SCSI summer 2018 sighting data

Table A.1: Summary of full summer sighting data by strata. Given is the number of unique groups sighted, number of groups sighted from the front position, number of groups sighted from the rear position and number of groups sighted from both positions (duplicates). Also given is the total number of individuals and average number of individuals per group. Naïve is the estimated number of dolphins assuming a strip transect survey with perfect detection and availability.

Coastal Section	Offshore Stratum (nmi)	Unique Groups	Front	Rear	Duplicates	Total Individuals	Average Group Size	Naïve
Te Waewae Bay	0–4	70	46	49	25	142	2.03	99
	4–12	5	5	3	3	12	2.40	10
Toetoes Bay	0–4	0	0	0	0	0	0	0
Elsewhere	0–4	0	0	0	0	0	0	0
	4–20	0	0	0	0	0	0	0
Total		**75**	**51**	**52**	**28**	**154**	**2.05**	**109**

SECTION B: Histograms of verified distance data for SCSI sightings

Figure B.1: Histogram of the verified distance data prior to any truncation of summer sightings from A) the front observer position, B) the rear observer position, and C) from either observer position in the summer survey. Grey bars indicate sightings made by both observers (duplicates).

A) Front Observer Detections

B) Rear Observer Detections

C) Combined Detections
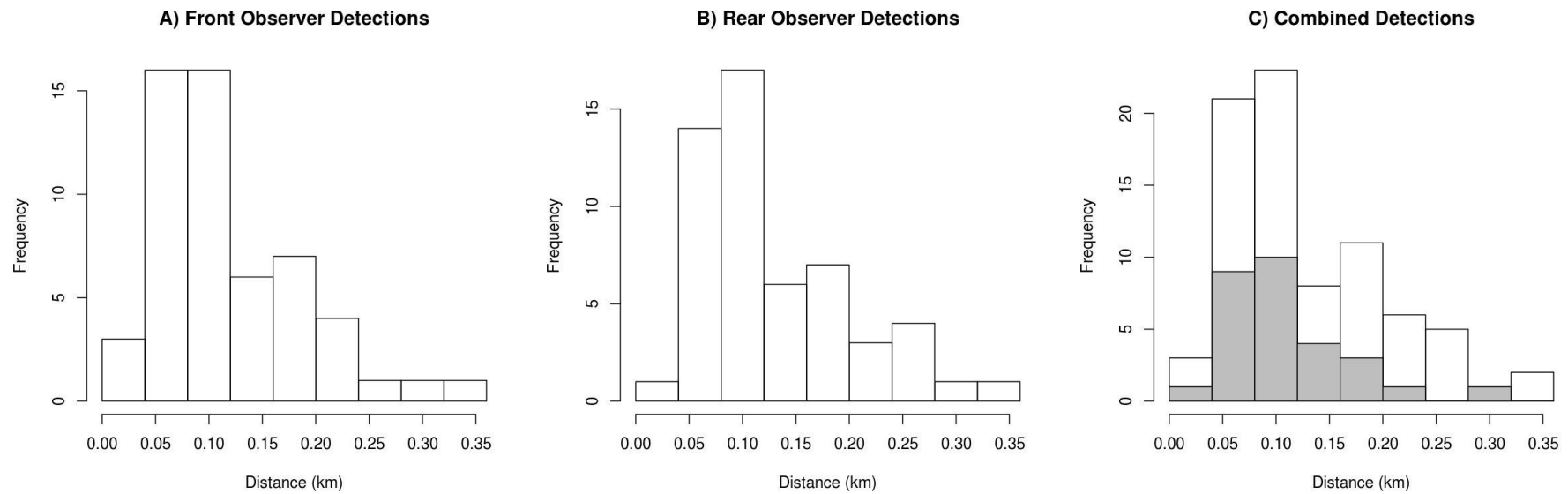
Figure B.2: Histogram of the distance data for sightings in the summer 2018 survey following left truncation at 0.040 km and right truncation at 0.300 km for both observer positions, from A) the front observer position, B) from the rear observer position, and C) either observer position. Grey bars indicate the number of sightings made by both observers (duplicates)
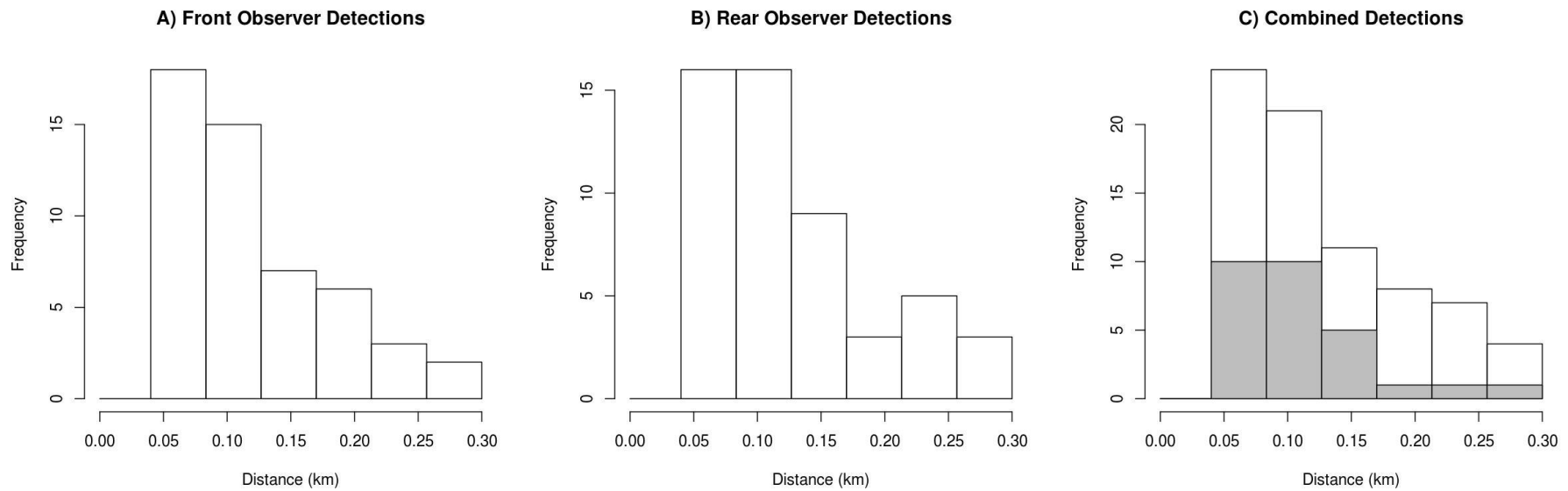
SECTION C: Diagnostic plots for detection function models fit

Figure C.1: Fitted detection functions and histograms of empirical detection probabilities from the top ranked model in Table 5. Left is $p_\bullet(d_i, s_i)$, centre is $p_F(d_i, s_i)$, and right is $p_R(d_i, s_i)$.
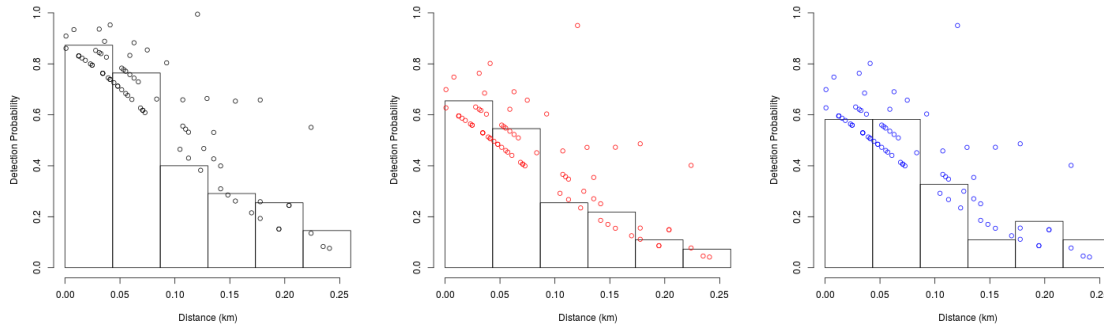

Figure C.2: Fitted detection functions and histograms of empirical detection probabilities from the second ranked model in Table 5. Left is $p_\bullet(d_i, s_i)$, centre is $p_F(d_i, s_i)$, and right is $p_R(d_i, s_i)$.
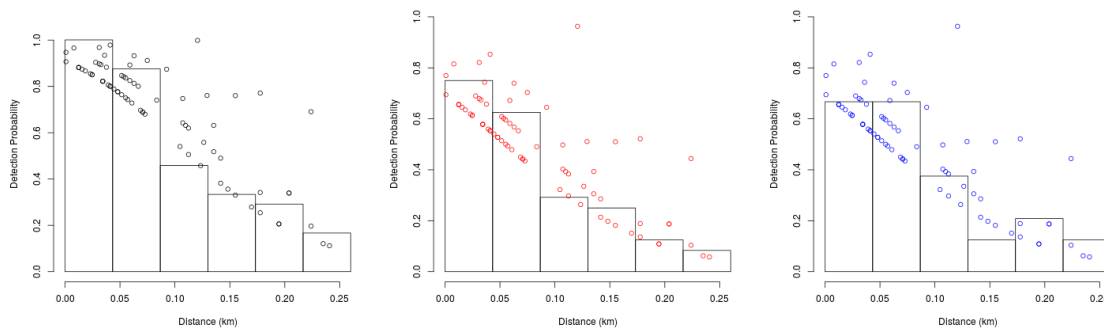
Figure C.3: Fitted detection functions and histograms of empirical detection probabilities from the third ranked model in Table 5. Left is $p_\bullet(d_i, s_i)$, centre is $p_F(d_i, s_i)$, and right is $p_R(d_i, s_i)$.
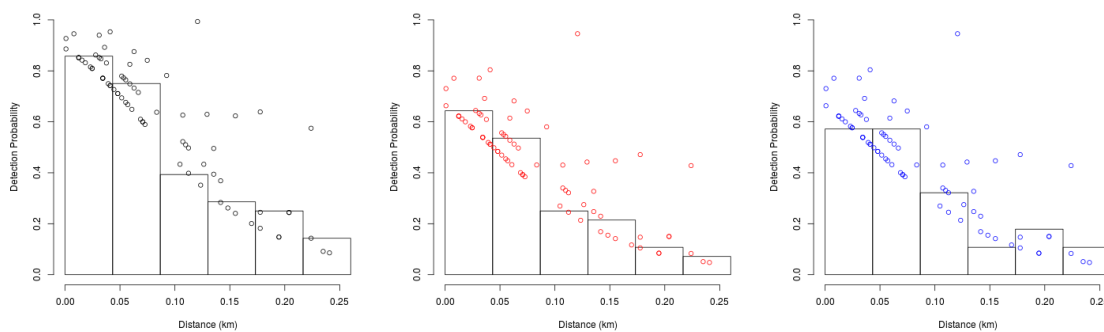
Figure C.4: Fitted detection functions and histograms of empirical detection probabilities from the fourth ranked model in Table 5. Left is $p_{\bullet}(d_i, s_i)$, centre is $p_F(d_i, s_i)$, and right is $p_R(d_i, s_i)$.
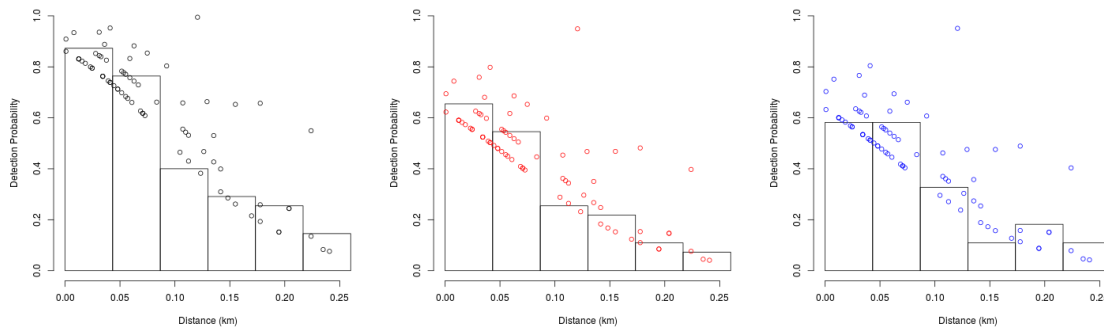
Figure C.5: Fitted detection functions and histograms of empirical detection probabilities from the fifth ranked model in Table 5. Left is $p_{\bullet}(d_i, s_i)$, centre is $p_F(d_i, s_i)$, and right is $p_R(d_i, s_i)$.
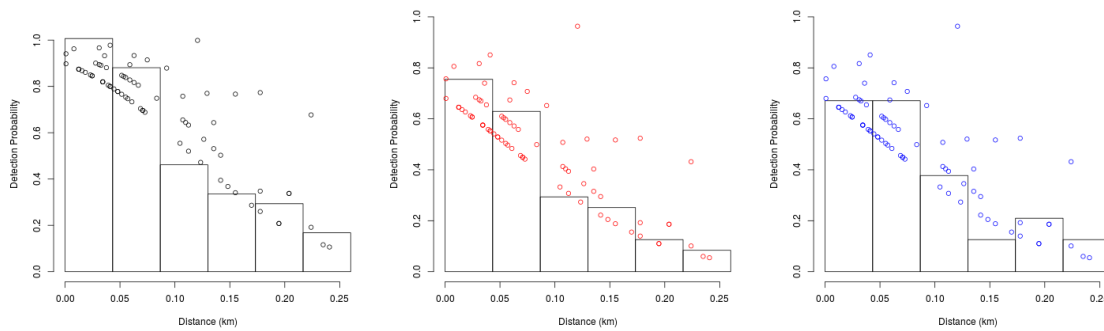

Figure C.6: Fitted detection functions and histograms of empirical detection probabilities from the sixth ranked model in Table 5. Left is $p_{\bullet}(d_i, s_i)$, centre is $p_F(d_i, s_i)$, and right is $p_R(d_i, s_i)$.
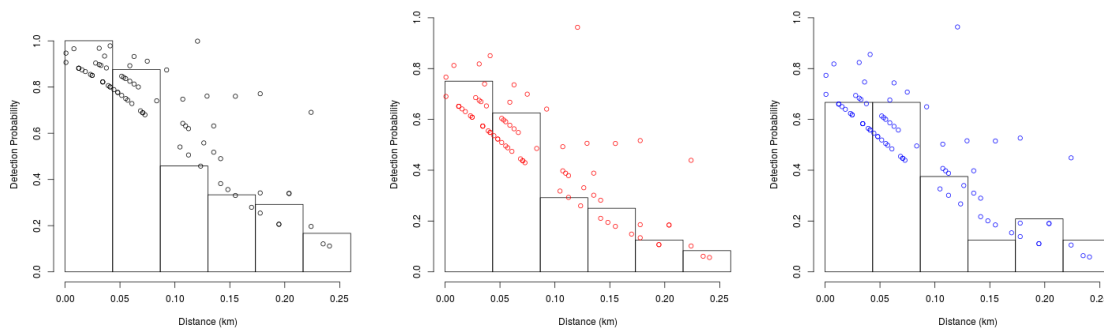
Figure C.7: Fitted detection functions and histograms of empirical detection probabilities from the seventh ranked model in Table 5. Left is $p_\bullet(d_i, s_i)$, centre is $p_F(d_i, s_i)$, and right is $p_R(d_i, s_i)$.
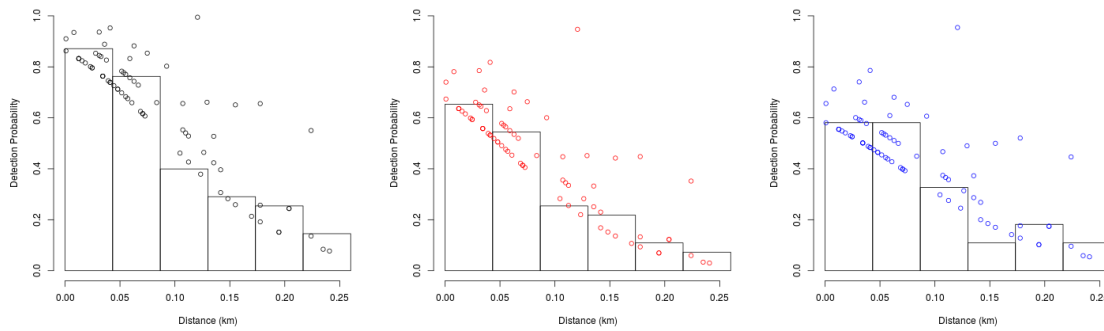
Figure C.8: Fitted detection functions and histograms of empirical detection probabilities from the eighth ranked model in Table 5. Left is $p_\bullet(d_i, s_i)$, centre is $p_F(d_i, s_i)$, and right is $p_R(d_i, s_i)$.
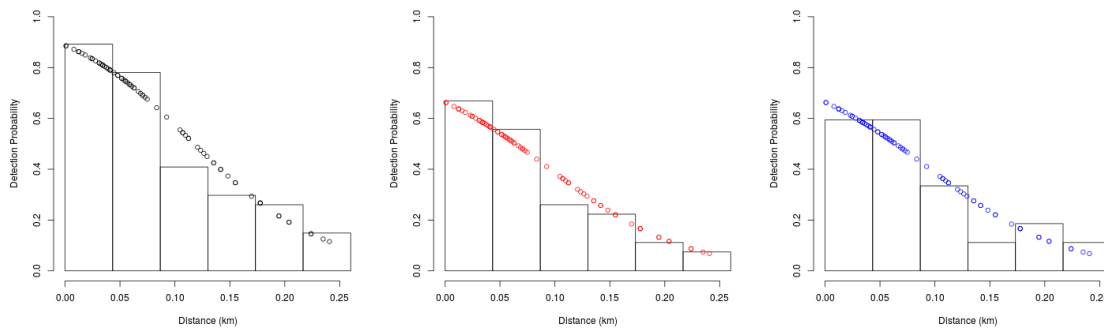
Figure C.9: Fitted detection functions and histograms of empirical detection probabilities from the ninth ranked model in Table 5. Left is $p_\bullet(d_i, s_i)$, centre is $p_F(d_i, s_i)$, and right is $p_R(d_i, s_i)$.
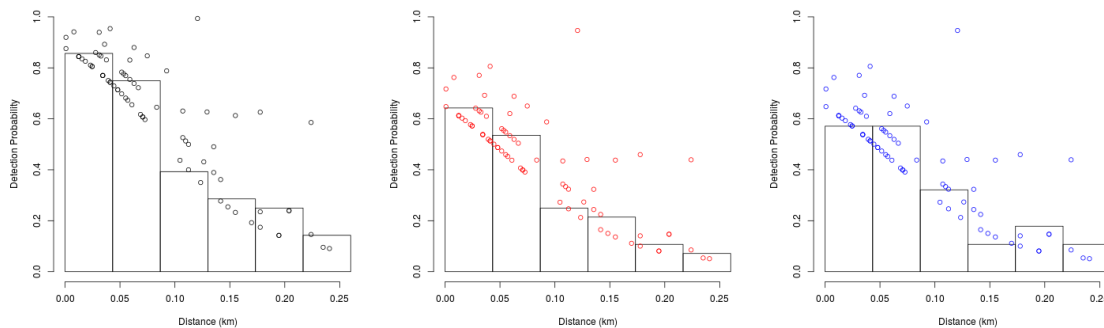
Figure C.10: Fitted detection functions and histograms of empirical detection probabilities from the tenth ranked model in Table 5. Left is $p_\bullet(d_i, s_i)$, **centre is** $p_F(d_i, s_i)$, **and right is** $p_R(d_i, s_i)$.
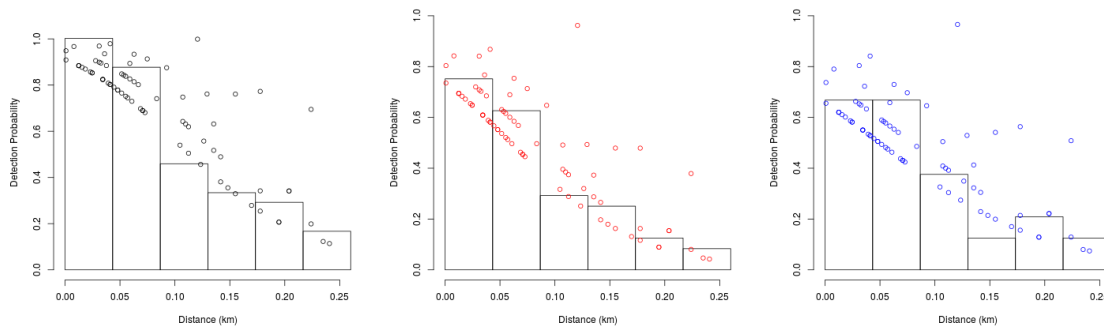
Figure C.11: Q-Q plot of the fitted and empirical cumulative density functions (CDF) for the top ranked model of the detection function analysis of the full summer data.
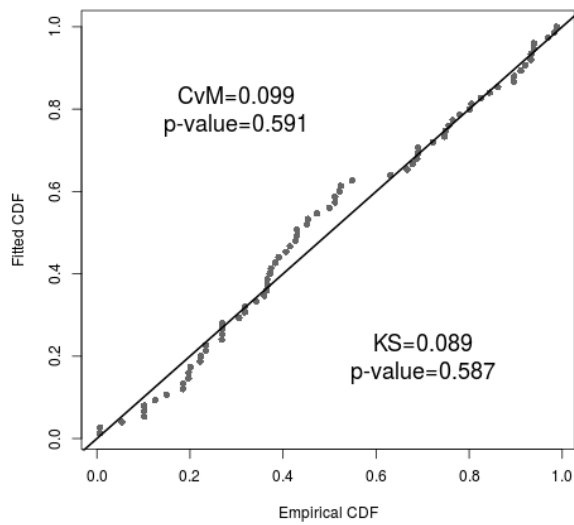
Figure C.12: Q-Q plot of the fitted and empirical cumulative density functions (CDF) for the second ranked model of the detection function analysis of the full summer data.
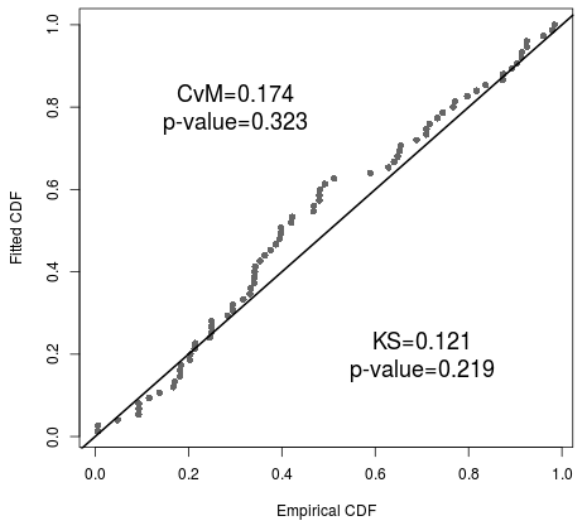
Figure C.13: Q-Q plot of the fitted and empirical cumulative density functions (CDF) for the third ranked model of the detection function analysis of the full summer data.
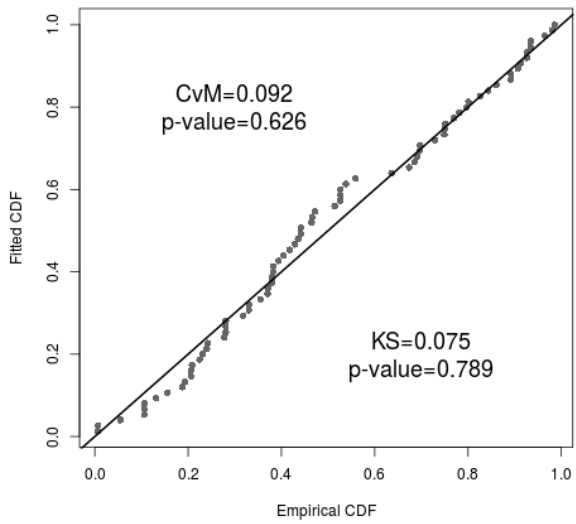
Figure C.14: Q-Q plot of the fitted and empirical cumulative density functions (CDF) for the fourth ranked model of the detection function analysis of the full summer data.
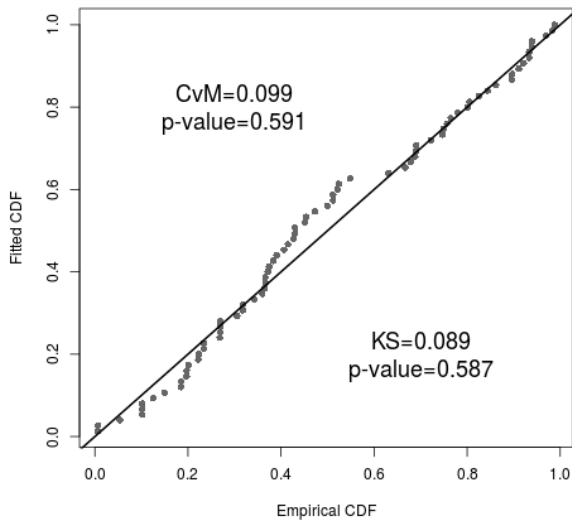

Figure C.15: Q-Q plot of the fitted and empirical cumulative density functions (CDF) for the fifth ranked model of the detection function analysis of the full summer data.
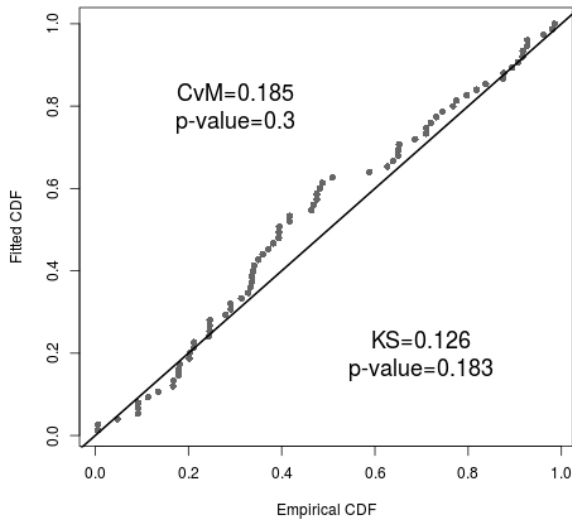
Figure C.16: Q-Q plot of the fitted and empirical cumulative density functions (CDF) for the sixth ranked model of the detection function analysis of the full summer data.
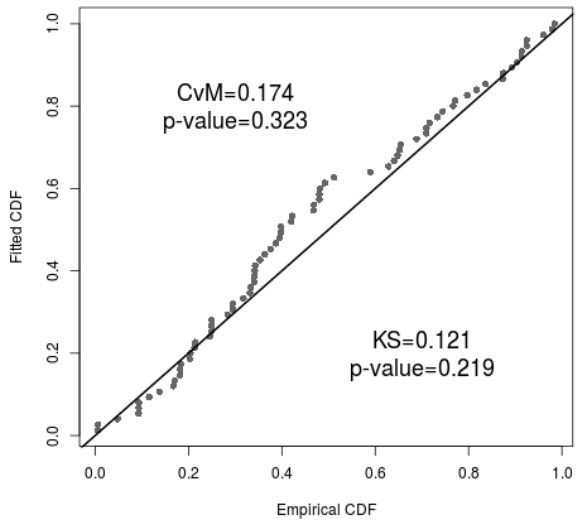

Figure C.17: Q-Q plot of the fitted and empirical cumulative density functions (CDF) for the seventh ranked model of the detection function analysis of the full summer data.
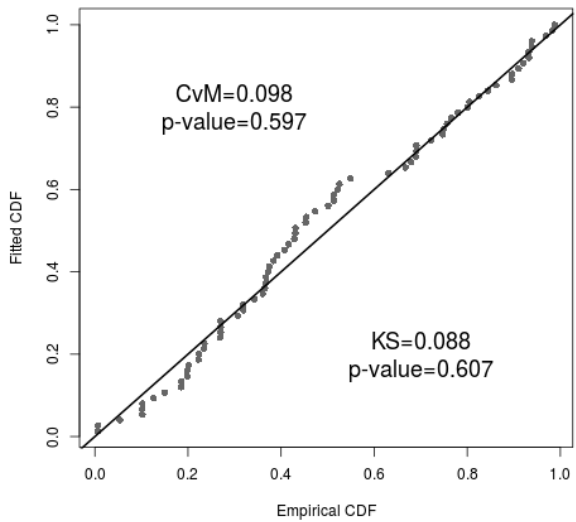
Figure C.18: Q-Q plot of the fitted and empirical cumulative density functions (CDF) for the eighth ranked model of the detection function analysis of the full summer data.
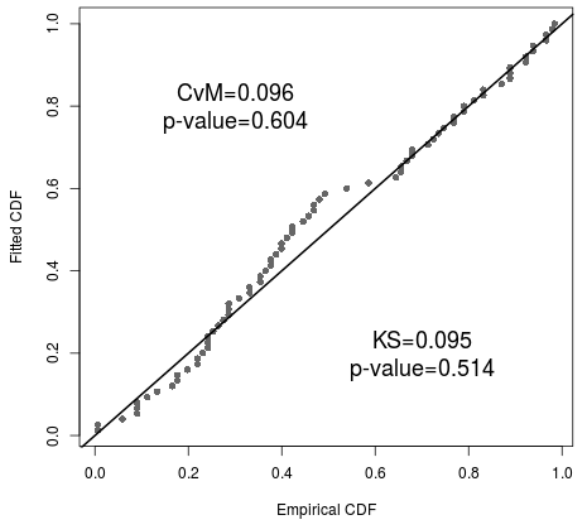
Figure C.19: Q-Q plot of the fitted and empirical cumulative density functions (CDF) for the ninth ranked model of the detection function analysis of the full summer data.
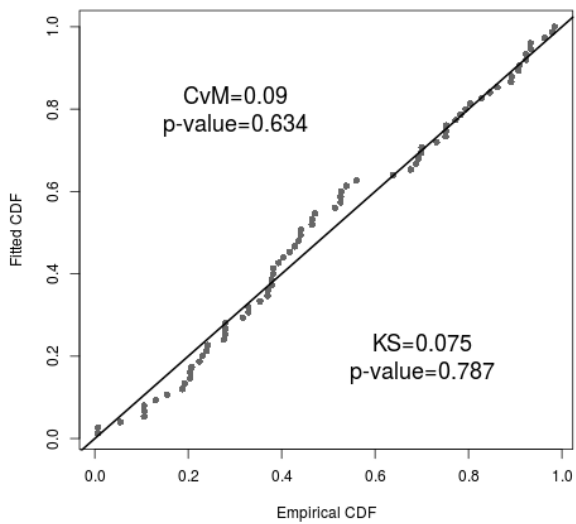
Figure C.20: Q-Q plot of the fitted and empirical cumulative density functions (CDF) for the tenth ranked model of the detection function analysis of the full summer data.
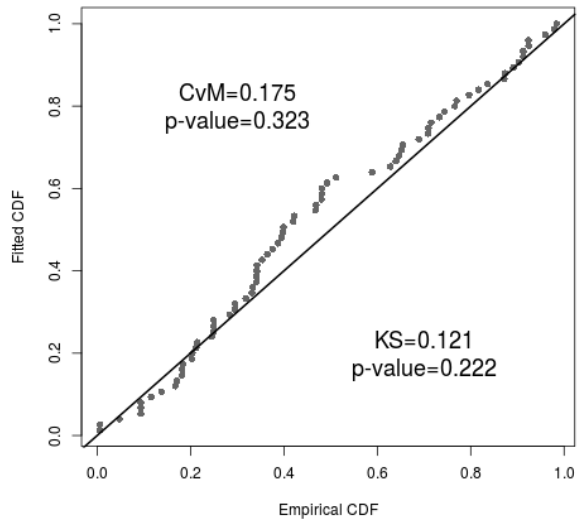
SECTION D: Stratum-specific SCSI summer abundance estimates.

Table D.1: Estimated summer abundance using the top ten models from Table 5 using the full sighting data and dive-cycle based availability estimates.

		Model 1		Model 2		Model 3		Model 4		Model 5	
Coastal Section	Offshore Stratum (nmi)	$\hat{N}_k$	SE	$\hat{N}_k$	SE	$\hat{N}_k$	SE	$\hat{N}_k$	SE	$\hat{N}_k$	SE
Te Waewae Bay	0–4	313	68	276	60	318	69	313	68	275	60
	4–12	32	12	28	10	32	12	32	12	28	10
Toetoe Bay	0–4										
Elsewhere	0–4										
	4–20										
Total		**345**	**71**	**304**	**62**	**350**	**72**	**345**	**71**	**302**	**62**

		Model 6		Model 7		Model 8		Model 9		Model 10	
Coastal Section	Offshore Stratum (nmi)	$\hat{N}_k$	SE	$\hat{N}_k$	SE	$\hat{N}_k$	SE	$\hat{N}_k$	SE	$\hat{N}_k$	SE
Te Waewae Bay	0–4	276	60	314	68	352	84	318	69	275	60
	4–12	28	10	32	12	36	14	32	12	28	10
Toetoes Bay	0–4										
Elsewhere	0–4										
	4–20										
Total		**304**	**62**	**345**	**71**	**388**	**87**	**350**	**72**	**303**	**62**